KBM Nonlinear Dynamics and First-Principles-Based Features in Deep Learning Algorithm for Predicting Disruptions

Ge Dong

Nov 20, 2018

Department of Astrophysical Sciences and Princeton Plasma Physics Laboratory,
Princeton, NJ 08543

Outline

Nonlinear KBM

- Introduction
- KBM saturation mechanism in Cyclone Base Case
- KBM nonlinear dynamics in DIII-D pedestal

Future work

- Motivation
- Feeding First-Principles-Based code output to AI

Ballooning mode as a candidate for explosive behavior in substorm onset

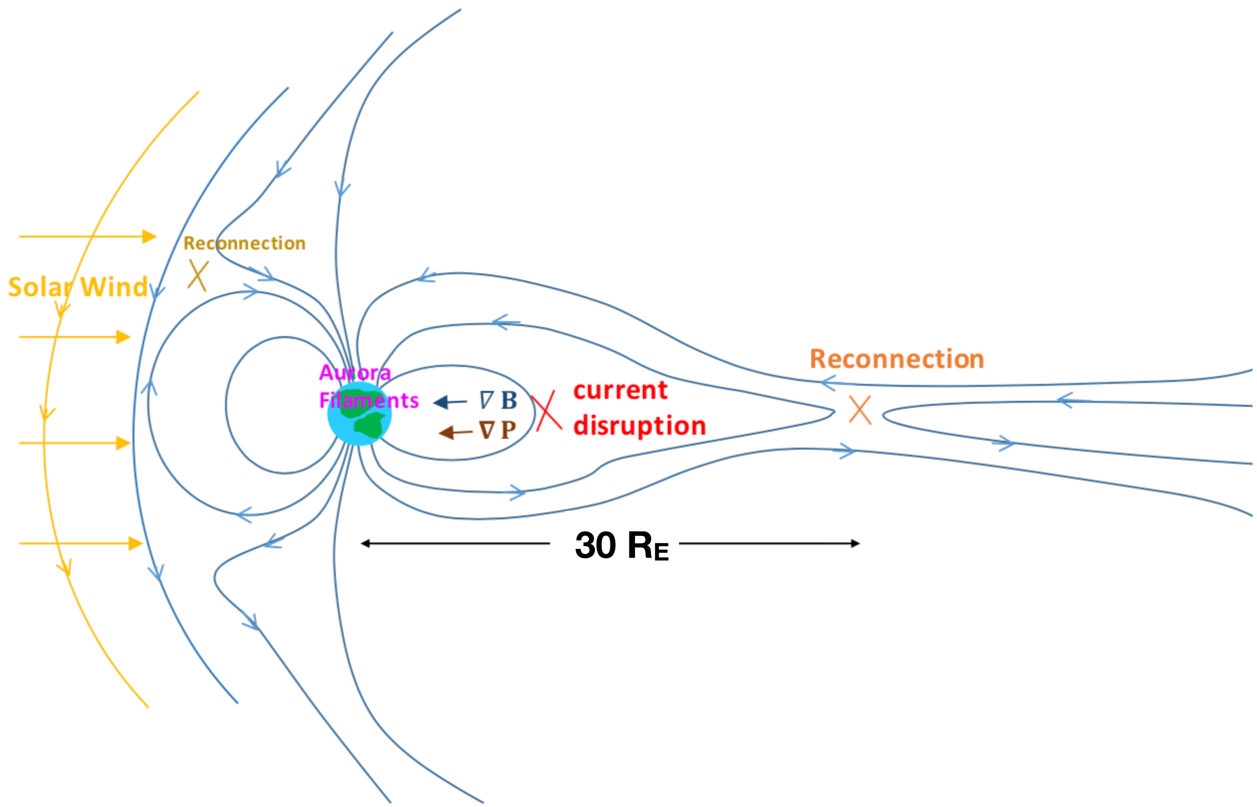

A Sketch of substorm onset.

Balloong modes are proposed as a candidate for triggering explosive behavior in substorm onset. [Bhattacharjee et al., 1998; Gohil et al., 1988; Raeder et al. 2010]

High frequency coherent fluctuations are related to ELM activities in various tokamak devices

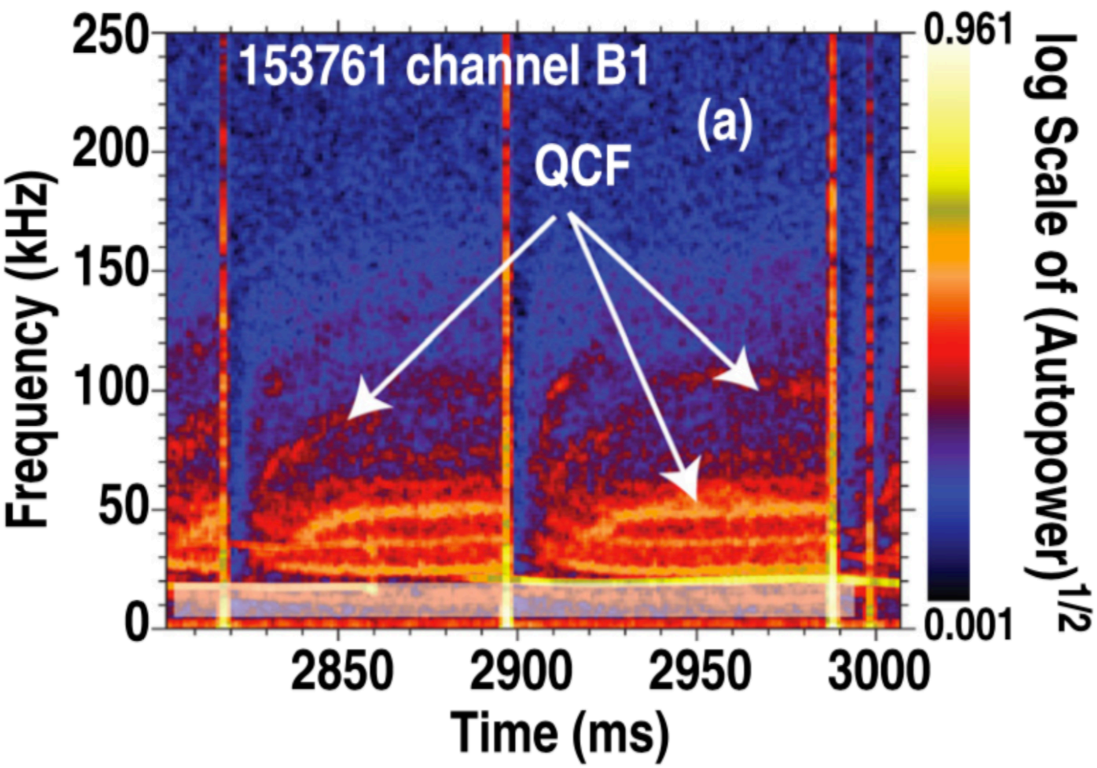

Quasi-coherent fluctuations and ELM crashes in DIII-D. Figure reproduced from *A. Diallo, Phys. Plasmas 22, 056111 (2015)*. Inter-ELM magnetic fluctuations spectrograms as measured using the Mirnov coils.

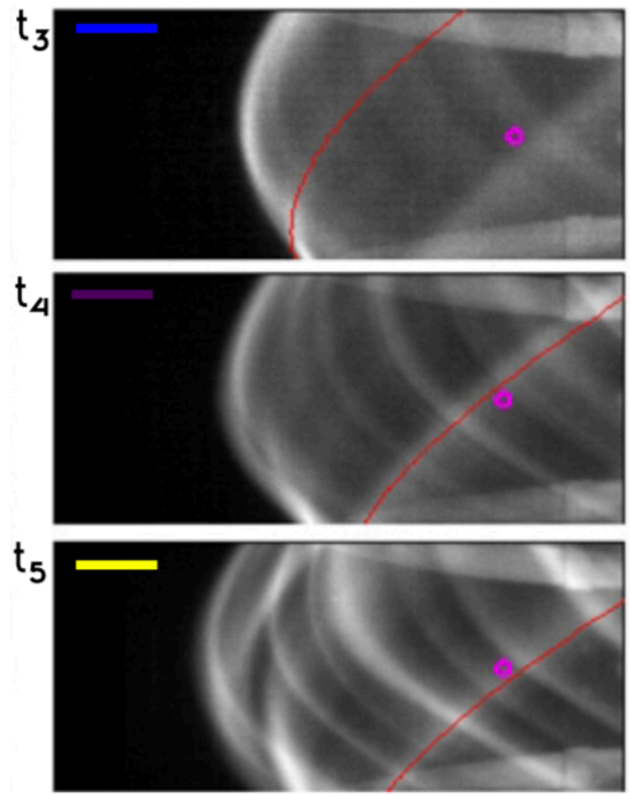

Filamentary structures of ELM on MAST. Figure reproduced from *R. Scannell, PPCF, 49, 1431, (2007)*. Filaments observed during an ELM by the Photron camera. The camera frames are separated by 16 μs

Explosive growth of IBM and the intermediate regime in MHD simulations

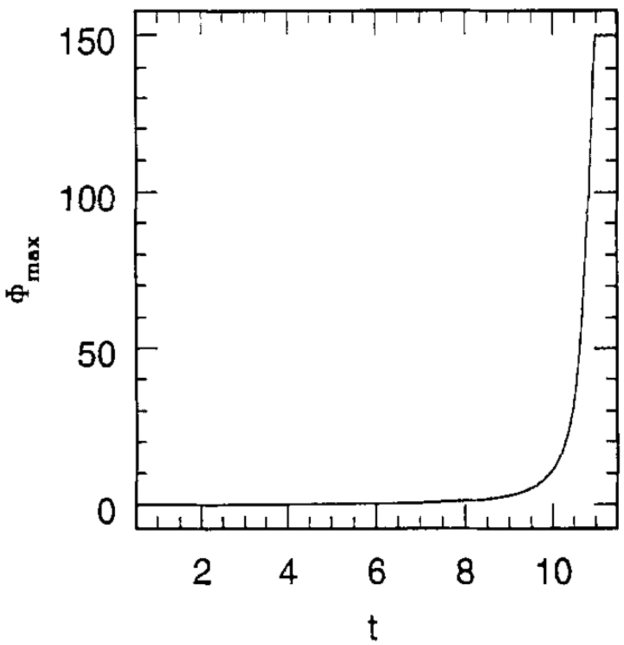

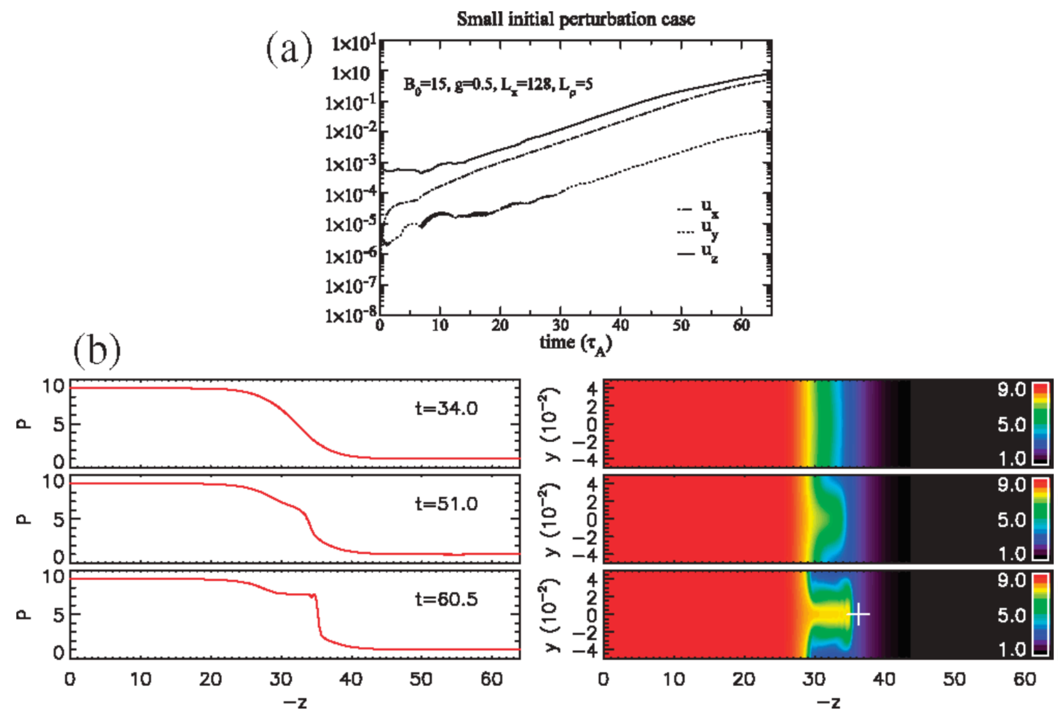

Finite time singularity of the flow poloidal gradient in ideal ballooning mode near marginal instability.
Figure reproduced from *S. C. Cowley, Physics Reports 283 (1997)*

Exponential nonlinear growth of weakly unstable ballooning modes in full MHD simulations.
Intermediate regime is formulated to describe the nonlinear behavior.
Figure reproduced from *P. Zhu, PRL 96, 065001 (2006)*

Gyrokinetic simulation model

Gyrokinetic ion model.
Solve Vlasov equation directly.

Conservative scheme for electrons.
Separate adiabatic $\delta f_e^{(a)}$ and non-adiabatic part δh_e.
Solve δn_e from continuity equation, then $\delta f_e^{(a)}$ analytically.

$$\frac{\partial \delta A_\parallel^A}{\partial t} = c\mathbf{b}_0 \cdot \nabla \phi_{ind}.$$

Adiabatic (non-tearing)
(No ``cancellation'' problem)

$$\frac{1}{c}\frac{\partial \delta A_\parallel^{na}}{\partial t} = \frac{\delta \mathbf{B}_\perp}{B_0} \cdot \nabla \delta \phi_{ind} - \frac{m_e}{n_0 e^2} \nabla \cdot \left(\delta u_{\parallel e} \frac{c P_{e0} \mathbf{B_0} \times \nabla \delta B_\parallel}{B_0^3} \right) + \frac{P_{e0}}{e n_0} \frac{\delta \mathbf{B}_\perp}{B_0^2} \cdot \nabla \delta B_\parallel$$

Non-adiabatic (includes tearing parity)

GTC Flow Chart-Conservative

$$\delta f_i^n,\ \delta n_e^n,\ \delta \phi^n,\ \delta \phi_{ind}^n,\ \delta A_\parallel^{A,n}$$
$$\delta A_\parallel^{NA,n},\ \delta B_\parallel^n,\ \delta h_e^n,\ \delta u_{e\parallel}^n$$

$$\delta f_i^{n+1} = \frac{\partial f_i}{\partial t}\left(\delta\phi^n, \delta\phi_{ind}^n, \delta B_\parallel^n, \delta A_\parallel^{A,n}, \delta A_\parallel^{NA,n}\right)\Delta t + \delta f_i^n$$

$$\delta n_e^{n+1} = \frac{\partial \delta n_e}{\partial t}\left(\delta u_{e\parallel}^n, \delta\phi^n, \delta\phi_{ind}^n, \delta B_\parallel^n, \delta A_\parallel^{A,n}, \delta A_\parallel^{NA,n}\right)\Delta t + \delta n_e^n$$

$$\delta A_\parallel^{A,n+1} = \frac{\partial \delta A_\parallel^A}{\partial t}\left(\delta\phi_{ind}^n\right)\Delta t + \delta A_\parallel^{A,n}$$

$$\delta A_\parallel^{NA,n+1} = \frac{\partial \delta A_\parallel^{NA}}{\partial t}\left(\delta u_{e\parallel}^n, \delta\phi^n, \delta\phi_{ind}^n, \delta B_\parallel^n, \delta A_\parallel^{A,n}, \delta A_\parallel^{NA,n}\right)\Delta t + \delta A_\parallel^{NA,n}$$

$$\delta h_e^{n+1} = \frac{\partial \delta h_e}{\partial t}\left(\frac{\partial \delta f_e^{(a),n}}{\partial t}, \delta\phi^n, \delta\phi_{ind}^n, \delta B_\parallel^n, \delta A_\parallel^{A,n}, \delta A_\parallel^{NA,n}\right)\Delta t + \delta h_e^n$$

$$\delta\phi_{ind}^{n+1} = \delta\phi_{ind}(\delta n^{n+1}, \delta\phi^{n+1}, \delta A_\parallel^{A,n+1})$$

$$\frac{\delta f^{(a),n+1}}{\partial t} = \frac{\delta f^{(a)}}{\partial t}\left(\frac{\partial \delta n_e^{n+1}}{\partial t}, \delta\phi_{ind}^{n+1}, \frac{\partial \delta B_\parallel^{n+1}}{\partial t}\right)$$

$$\delta u_{e\parallel}^{n+1} = \delta u_{e\parallel}(\delta A_\parallel^{A,n+1}, \delta A_\parallel^{NA,n+1}, \delta u_{i\parallel}^{n+1})$$

$$\delta B_\parallel^{n+1} = \delta B_\parallel(\delta P_e^{n+1}, \delta P_i^{n+1}, \delta\phi^{n+1})$$

$$\delta\phi^{n+1} = \delta\phi(\delta n_e^{n+1}, \delta n_i^{n+1}, \delta B_\parallel^{n+1})$$

Coupled Equation

$$\delta f_i^{n+1},\ \delta n_e^{n+1},\ \delta \phi^{n+1},\ \delta \phi_{ind}^{n+1},\ \delta A_\parallel^{A,n+1}$$
$$\delta A_\parallel^{NA,n+1},\ \delta B_\parallel^{n+1},\ \delta h_e^{n+1},\ \delta u_{e\parallel}^{n+1}$$

Gyrokinetic simulation model

Gyrokinetic Poisson Equation
And Perpendicular Ampere's Law

$$\frac{Z_i^2 n_i}{T_i}\left(\delta\phi - \tilde{\delta\phi}\right) - \frac{1}{B_0}\left(Z_i n_{i0}\{\delta B_\parallel\}_i - e n_{e0}\{\delta B_\parallel\}_e\right) = Z_i n_i - e n_e,$$

$$\begin{aligned}\frac{\delta B_\parallel B_0}{4\pi} &+ 2\pi\Omega_e^2 \int d\mu dv_\parallel \left[B_0 \left\langle \int_0^{\rho_e} F_e^{gyro} r dr \right\rangle + \frac{f_M}{\rho_e^2}\left\langle \int_0^{\rho_e} \left\langle \int_0^{\rho_e} \delta B_\parallel r' dr' \right\rangle r dr \right\rangle\right] \\ &= -2\pi\Omega_i^2 \int d\mu dv_\parallel \left[B_0 \left\langle \int_0^{\rho_i} \left(F_i^{gyro} + \frac{e\langle\delta\phi\rangle - e\delta\phi}{T_i} F_M\right) r dr \right\rangle + \frac{F_M}{\rho_i^2}\left\langle \int_0^{\rho_i} \left\langle \int_0^{\rho_i} \delta B_\parallel r' dr' \right\rangle r dr \right\rangle\right]. \qquad (12)\end{aligned}$$

$$\tilde{\delta\phi} = \int d\mathbf{v} \int d\mathbf{R} \langle\delta\phi\rangle(\mathbf{R}) F_M(\mathbf{R}, v_\parallel, \mu, t)\delta(\mathbf{x} - \mathbf{R} - \rho),$$

$$\{\delta B_\parallel\}_s = \frac{m\Omega_s^2}{2\pi T_s}\int d\mathbf{v} \int d\mathbf{R} \int_0^{\rho} r' dr' \int_0^{2\pi} d\zeta' \int d\mathbf{x}' \delta B_\parallel(\mathbf{x}') \times \delta(\mathbf{x}' - \mathbf{R} - \rho) F_M \delta(\mathbf{x} - \mathbf{R} - \rho).$$

GTC Flow Chart-Conservative

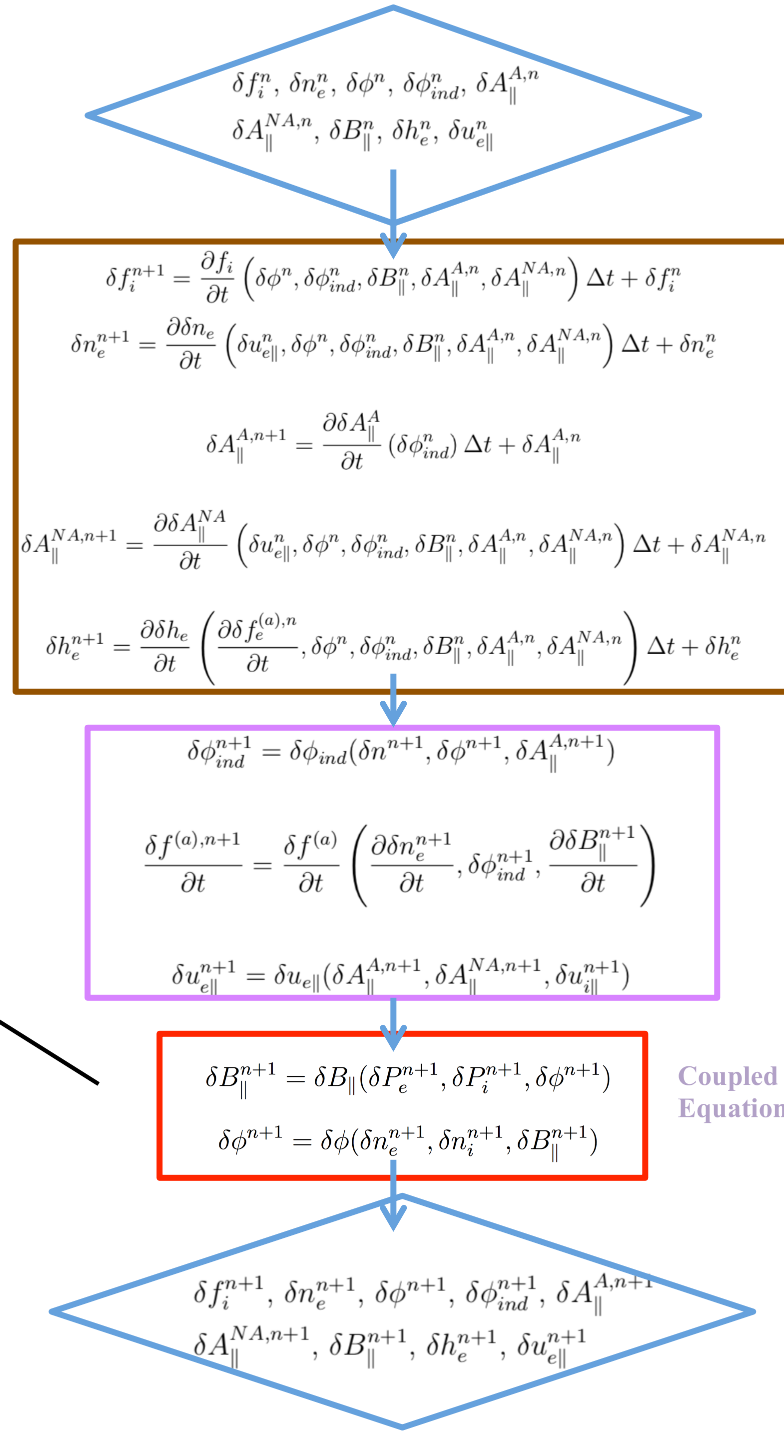

Spontaneous zonal flow generation

$$\phi_0(\mathbf{r},t)=e^{-i(n\phi+\omega_0 t)}\sum_m \Phi_0(m-nq)e^{im\theta},$$

$$\delta\phi_\pm=e^{i(\mp n\phi-(\omega_z\pm\omega_0)t+K_z r)}\sum_m \Phi_\pm(m-nq)e^{im\theta},$$

$$\delta\phi_z=\Phi_z e^{i(K_z r-\omega_z t)}+\text{c.c.}.$$

Gamma3~ $\nu_z=(1.5\epsilon\tau_{ii})^{-1}$

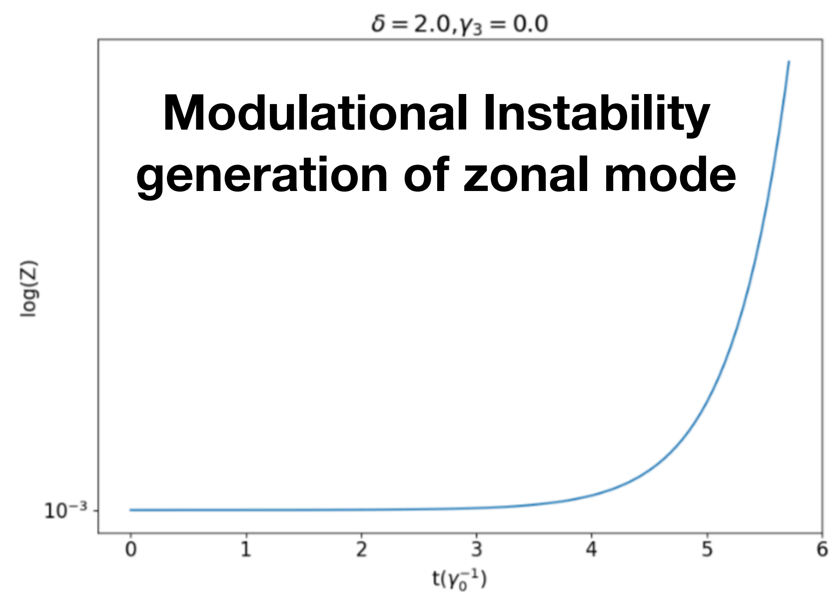

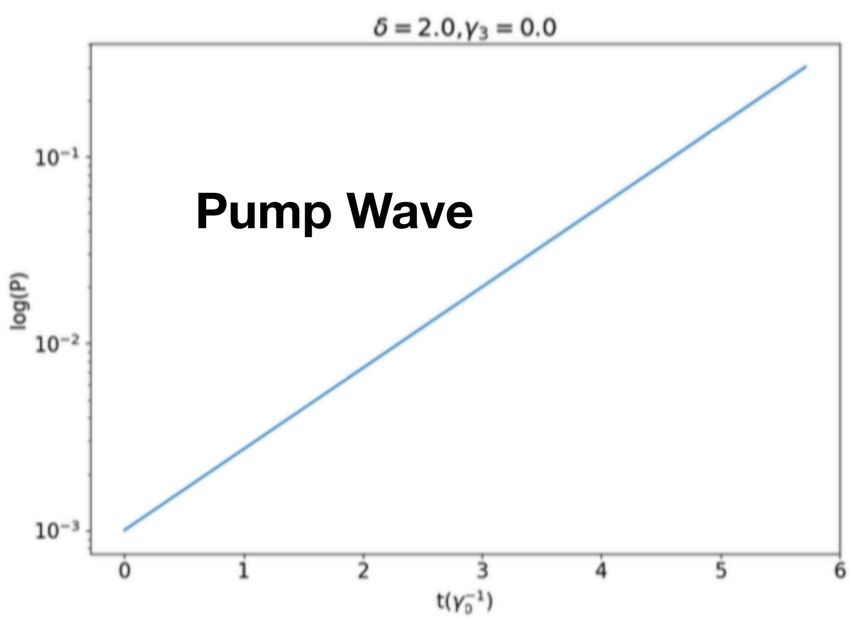

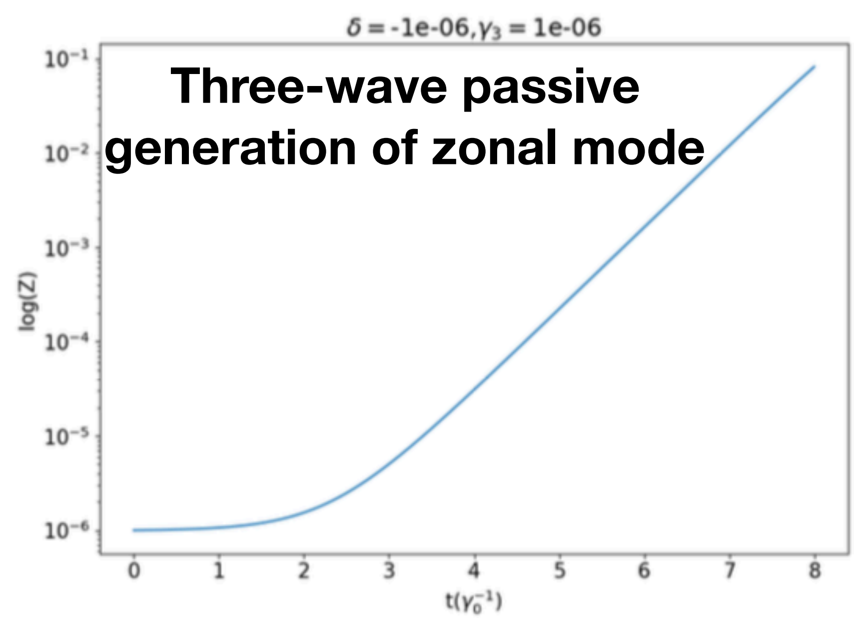

Route to Chaos

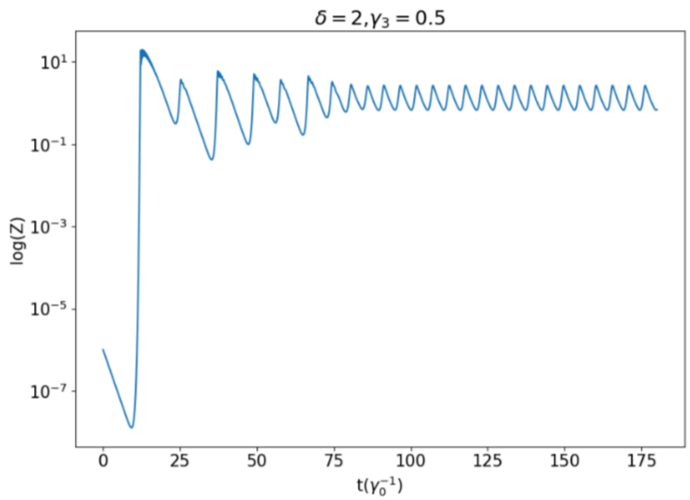

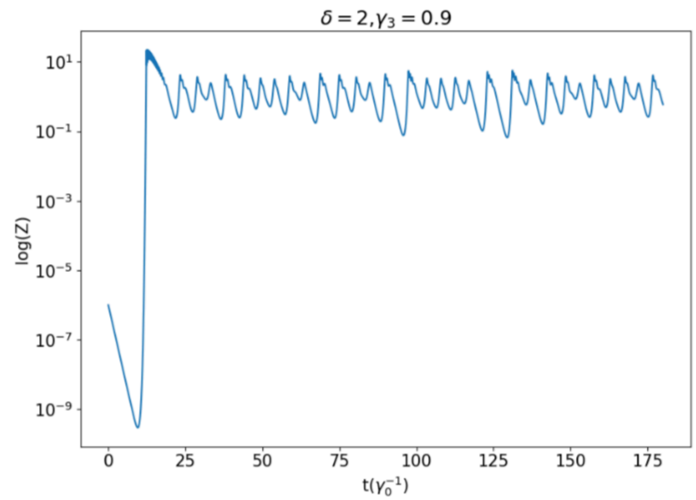

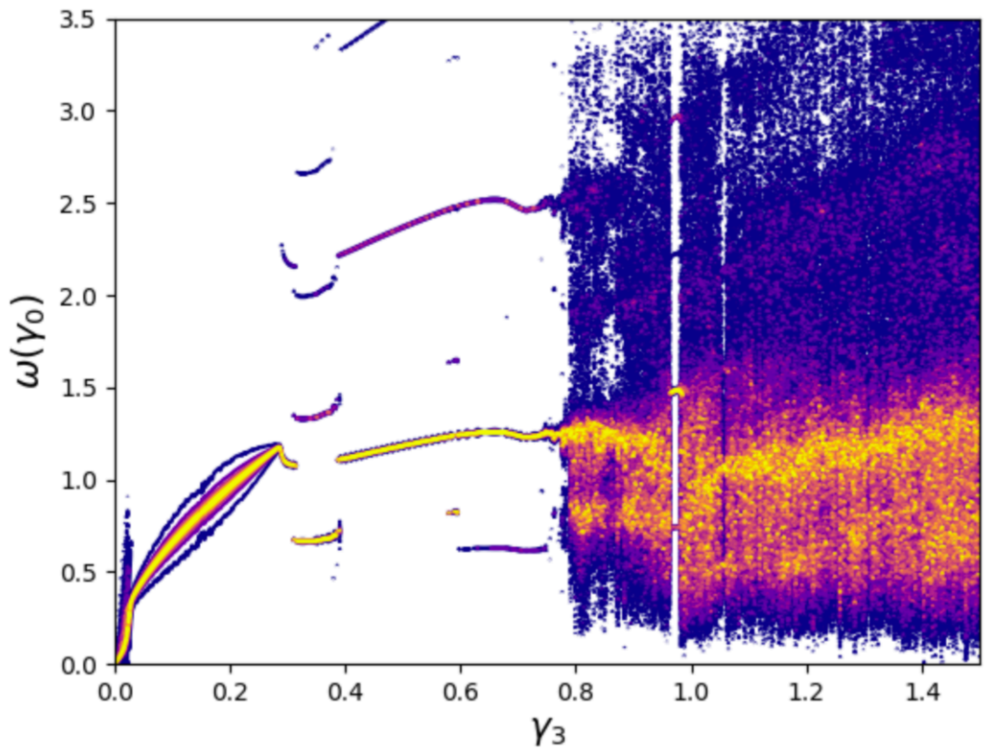

Zonal fields Saturation of KBM in Cyclone Base Case in global Gyrokinetic simulations

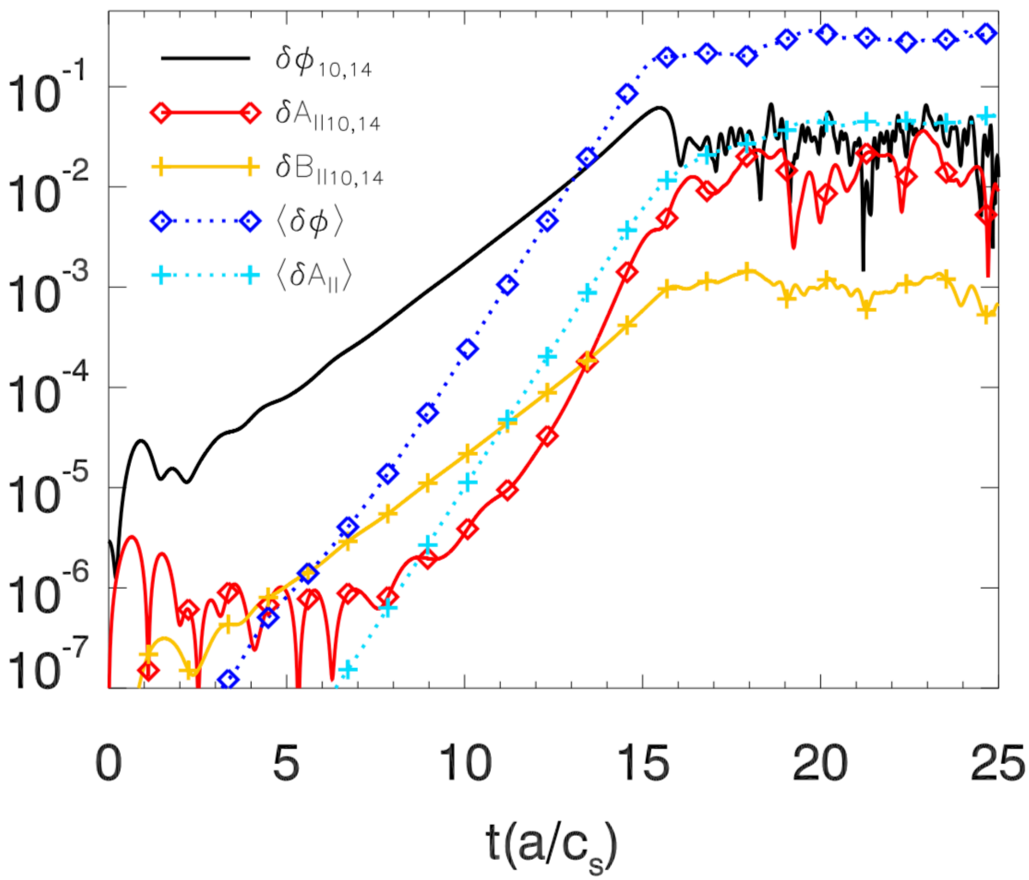

KBM nonlinear time history

Fixed equilibrium ∇P_0.

IBM unstable

CBC parameter: $R_0 = 83.5$cm, $a/R_0 = 0.357$. At $r = 0.5a$, $B_0 = 2.01$T , $T_e = 2223$eV , $R_0/L_T = 6.9$, $R_0/L_n = 2.2$, $q = 1.4$, $\beta_e = 2\%$.

First order $s - \alpha$ model with circular cross-section $\theta = \theta_0 - \varepsilon \sin\theta_0 + O(\varepsilon^2)$

Comparison of ITG and KBM zonal flow generation

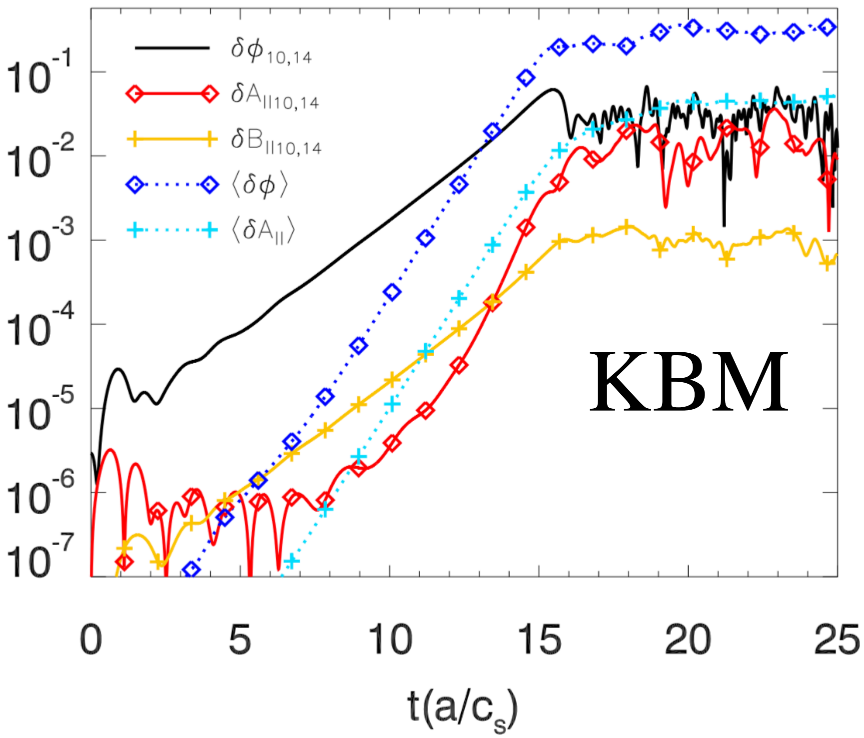

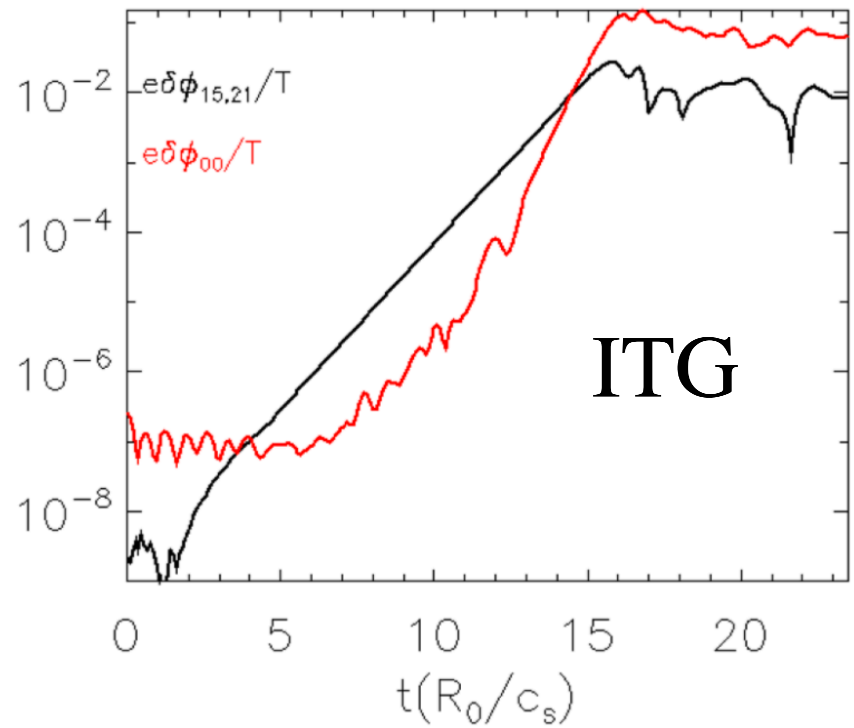

Zonal fields regulate mode saturation

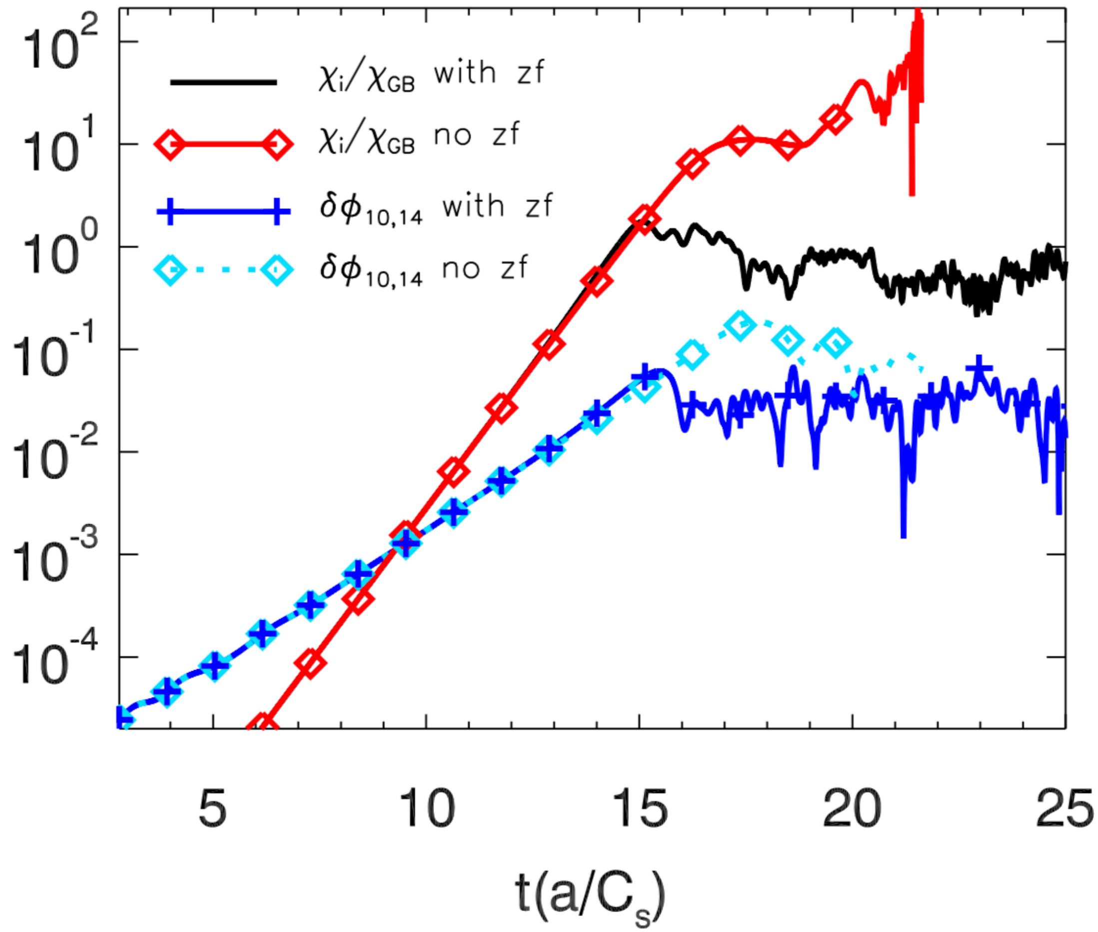

$$\chi_i = \frac{1}{n_0 \nabla T_i} \int d\mathbf{v} (\tfrac{1}{2} m_i v^2 - \tfrac{3}{2} T_i) v_r \delta f$$

Comparison of simulation with and w/o zonal fields.
In the case w/o zonal fields, the mode saturates at almost one order of magnitude higher

Both the Zonal flow and Zonal Current are important

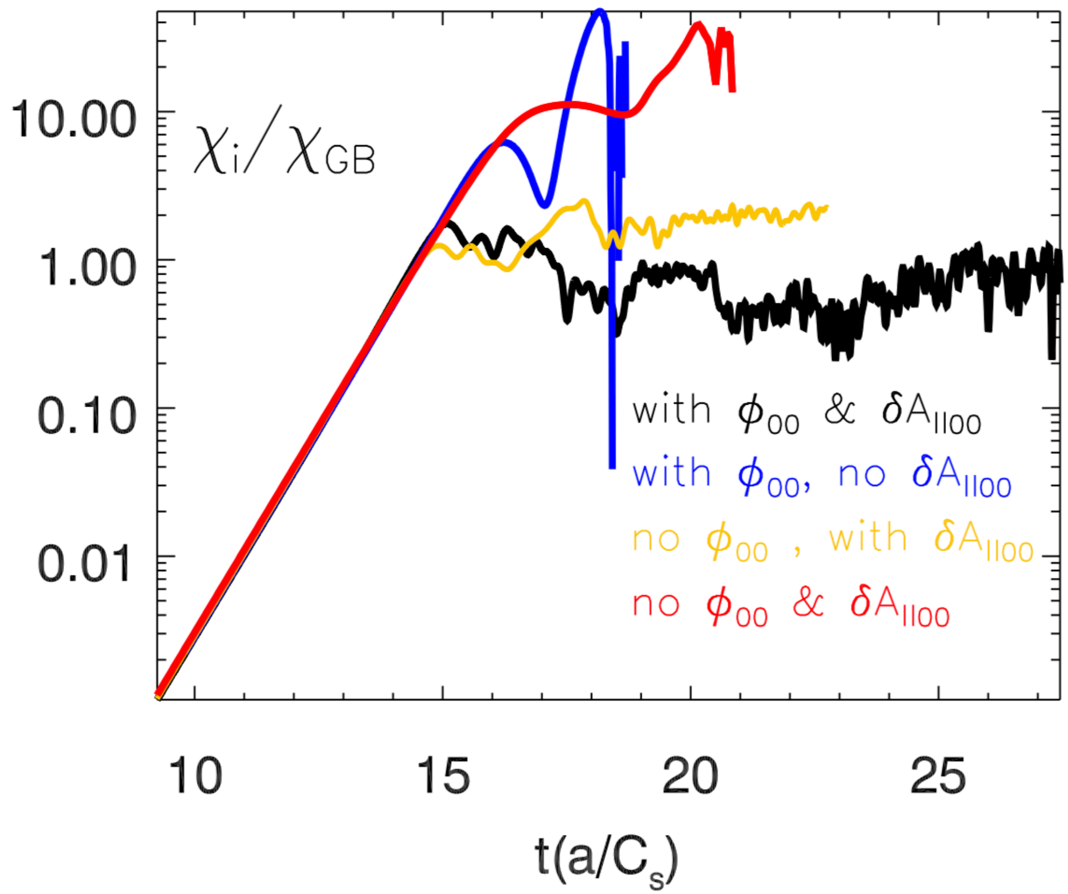

Comparison of 4 simulation with and w/o zonal current/ zonal flow respectively.

Zonal fields breaking of mode structure

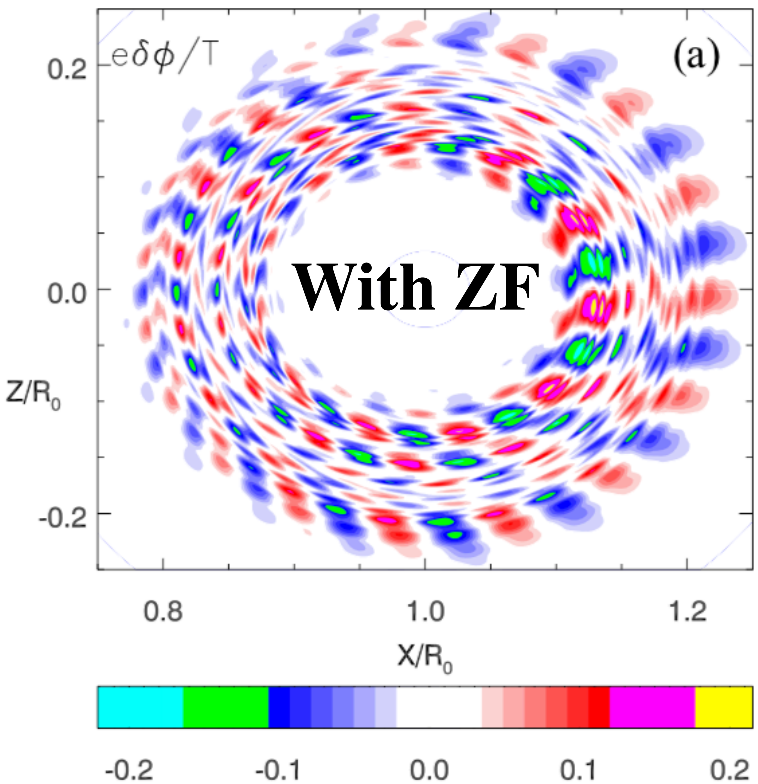

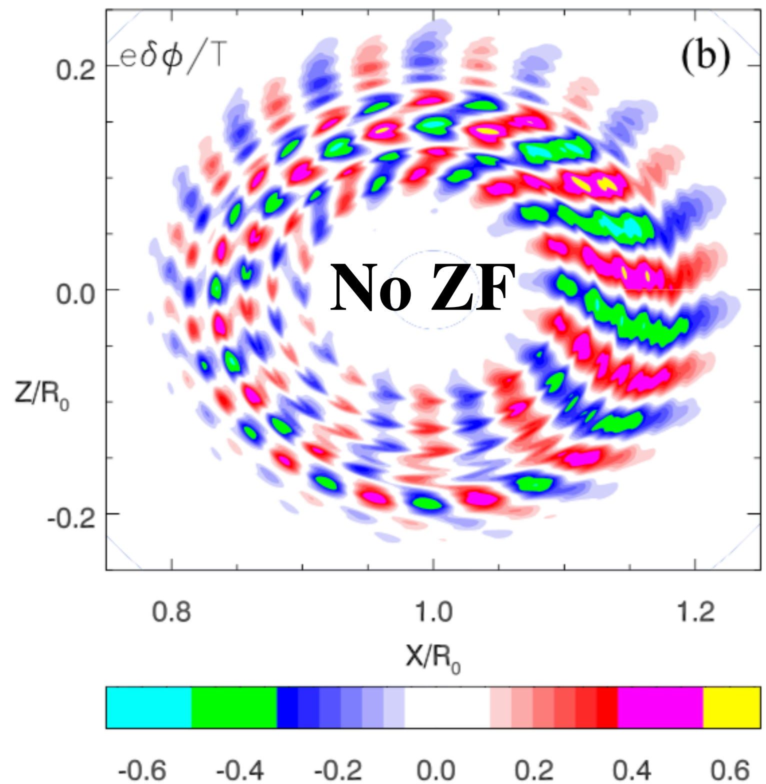

Broken radial filaments with self-consistently generated zonal flow and zonal current.

Macroscale radial filaments in the simulation without zonal fields.

Generation of high n localized current sheet

Non-tearing mode nonlinearly can induce tearing mode

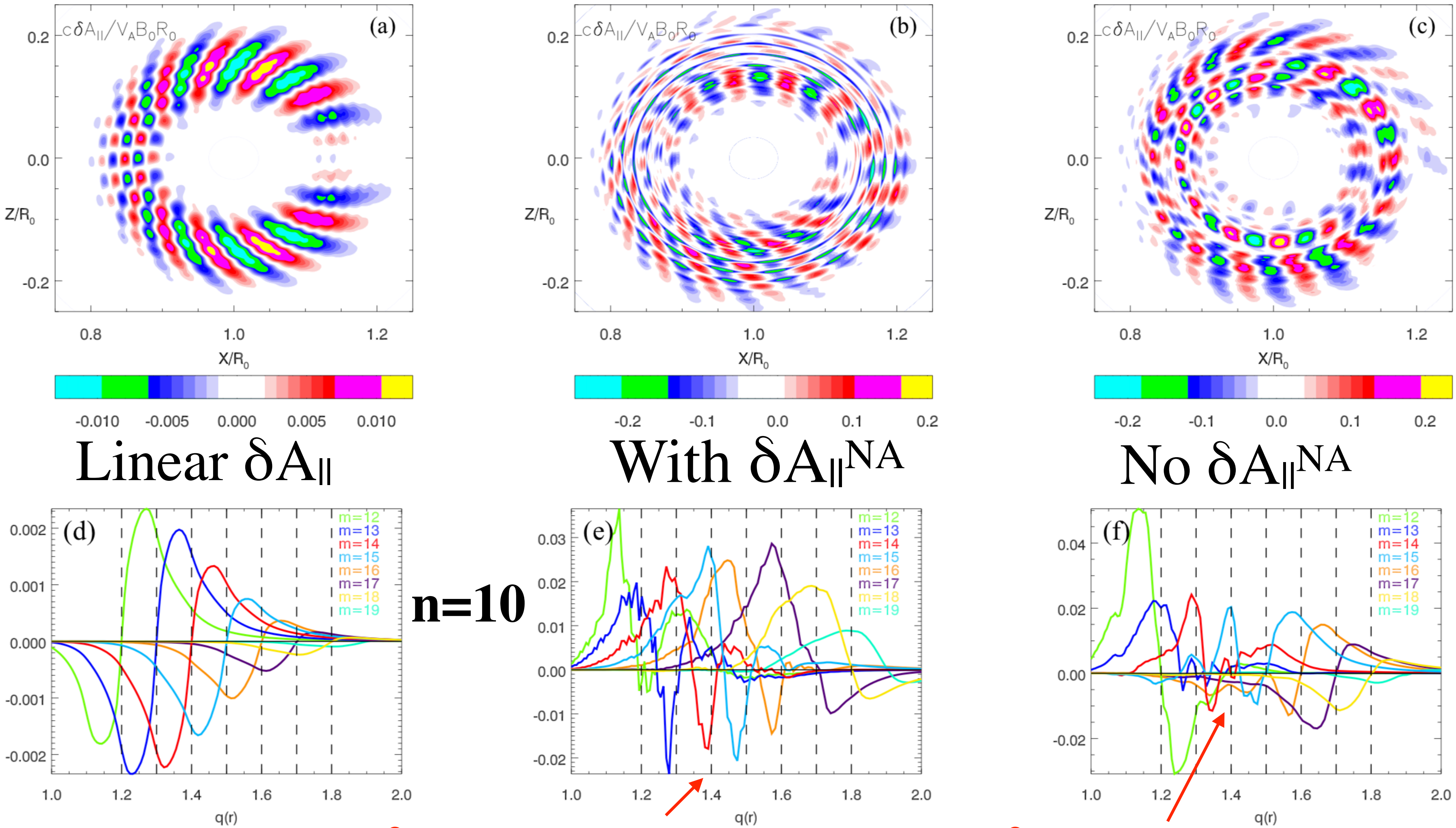

$\delta A_{\parallel}$ finite at Rational Surface **$\delta A_{\parallel}$=0 at RS**

Saturation mechanism not sensitive to β_e

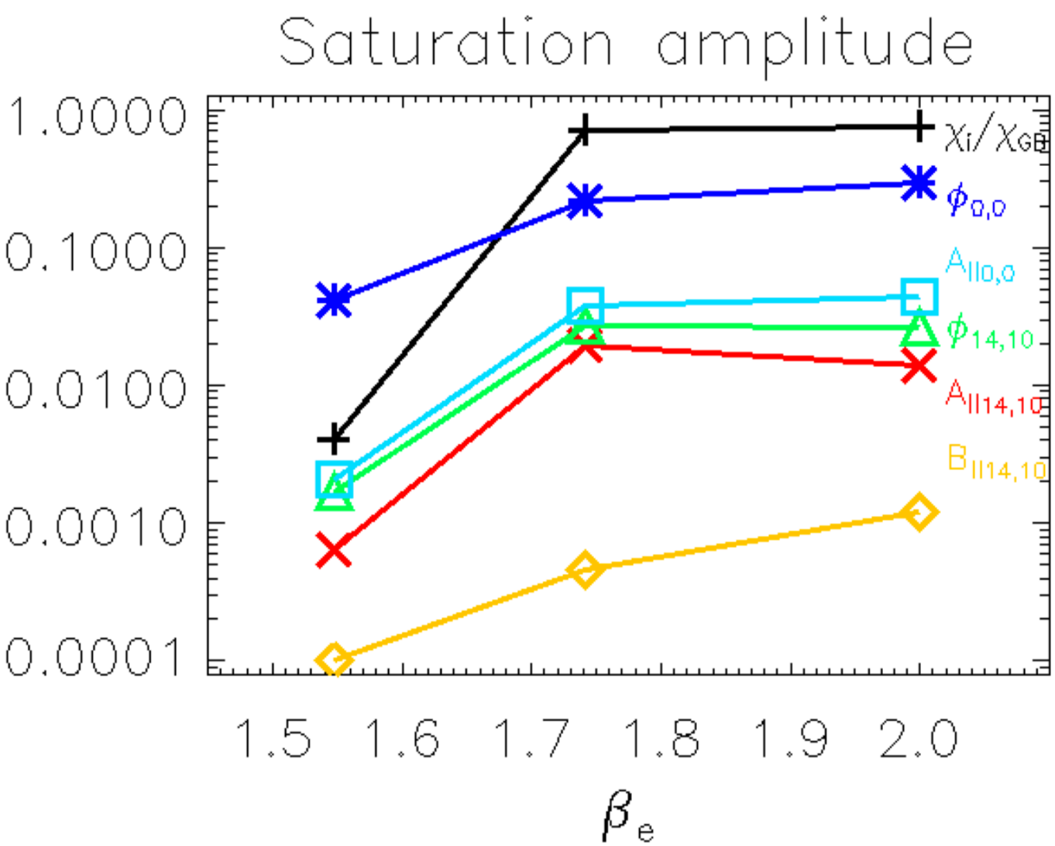

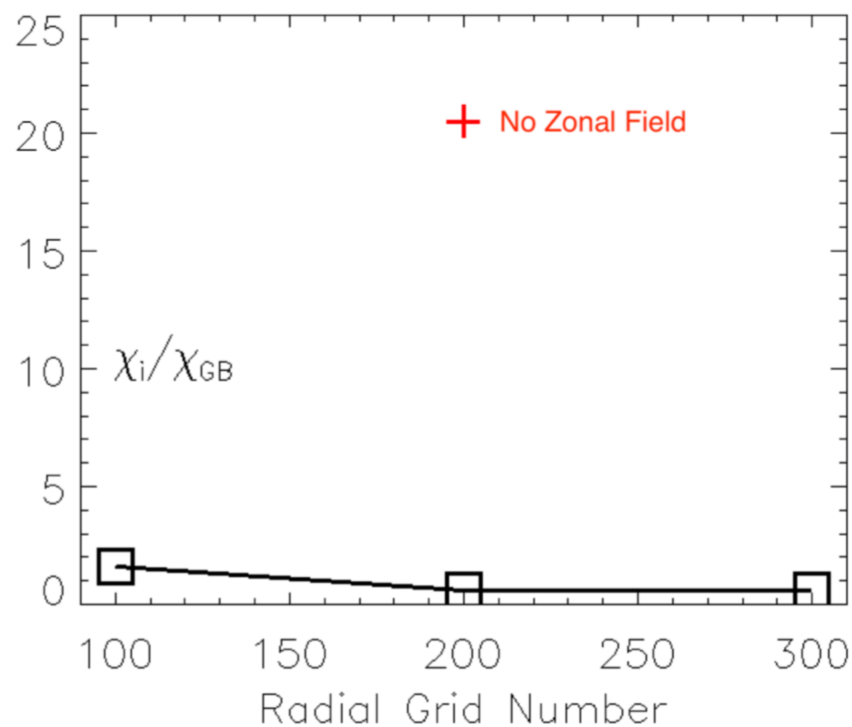

Similar saturation features for lower β_e

Convergence study

KBM in DIII-D pedestal steep gradient region

Table 4.1: Parameter for DIII-D shot #145701 at the steep gradient region at $\psi_n = 0.985$

T_e	T_i	n_e	L_n/L_{Ti}	R_0/L_n	R_0/L_{Te}	R_0/L_{Ti}	q	β_e
$197ev$	$396ev$	$2.48 \times 10^{19} m^{-3}$	0.13	64	144	8	0.36	0.7%

No equilibrium E_r shear

Collisionless

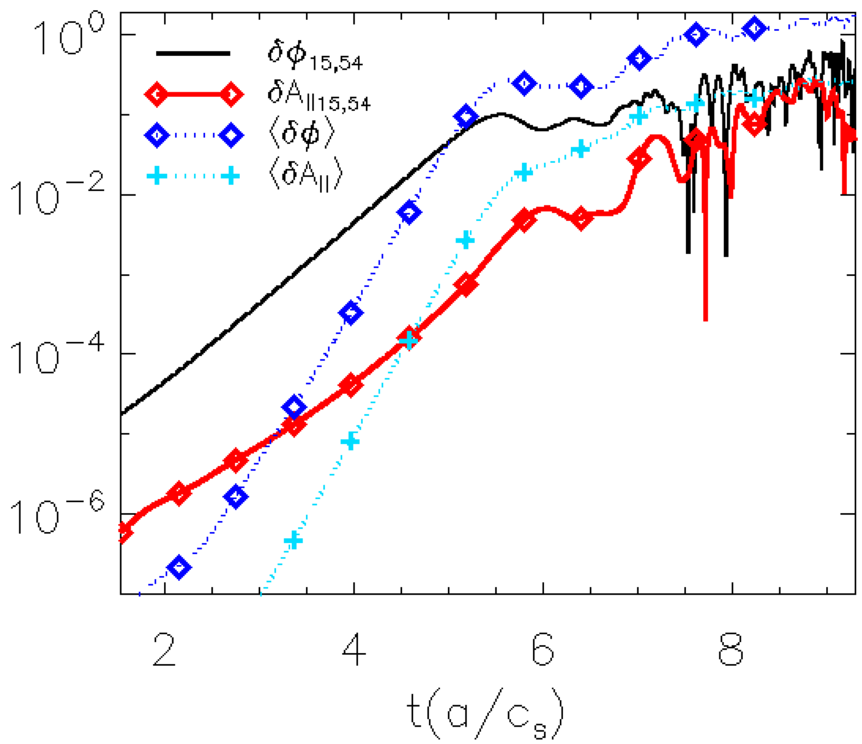

Time history of nonlinear mode evolution for KBM in DIII-D edge

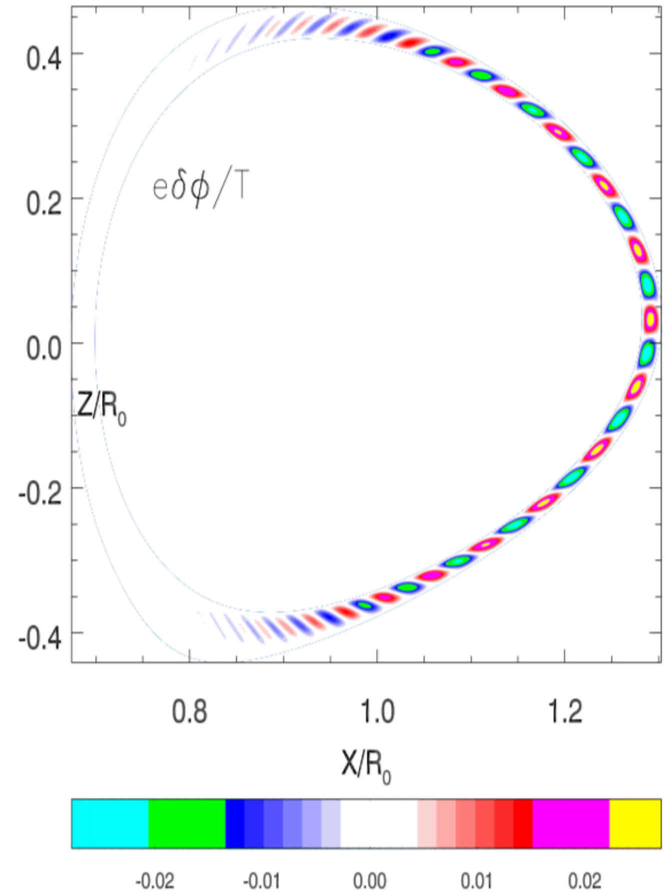

Linear mode structure

Competing effects of ZF and the ExB convection

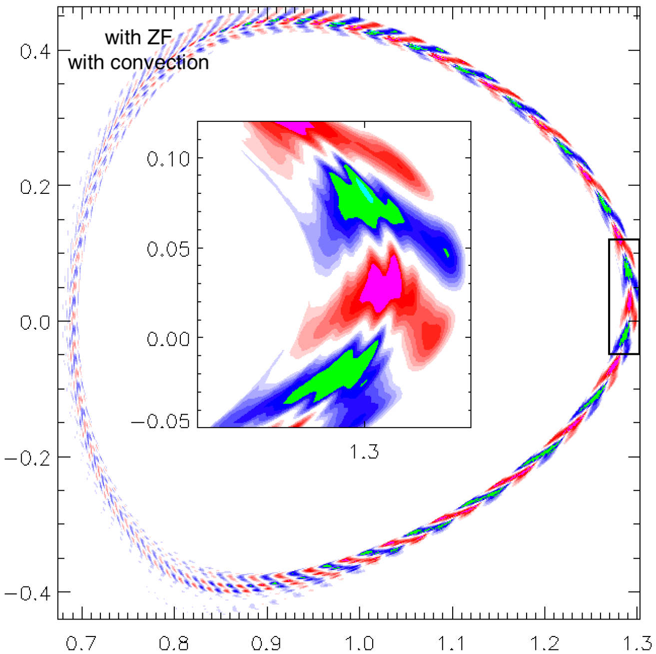

Nonlinear KBM $\delta\phi$

poloidal contour

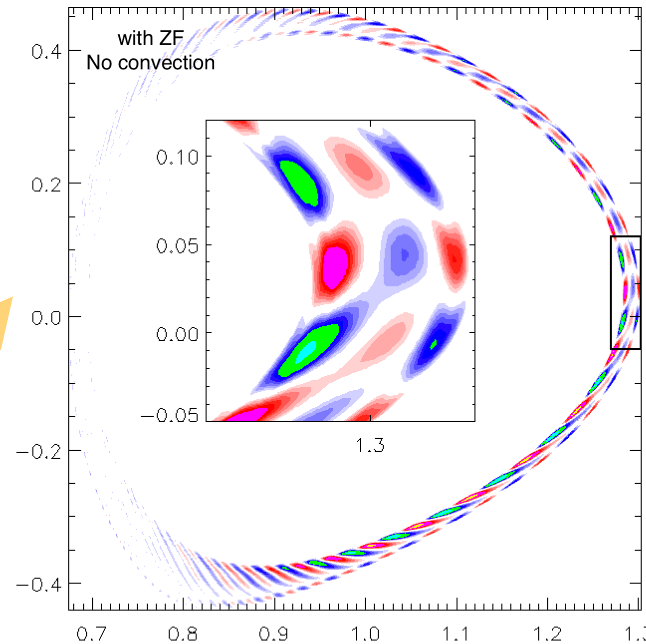

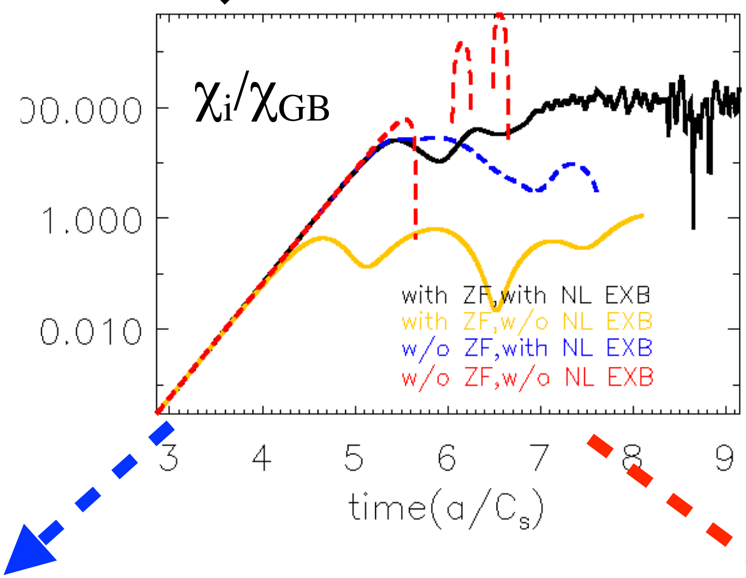

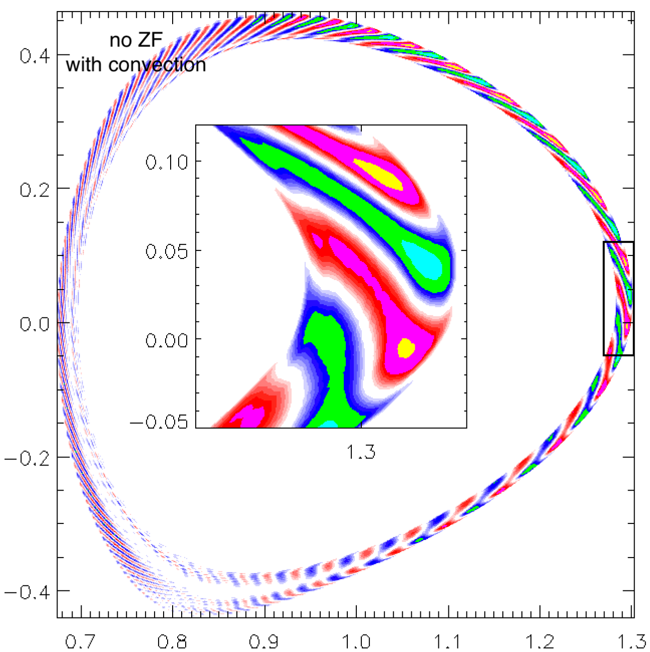

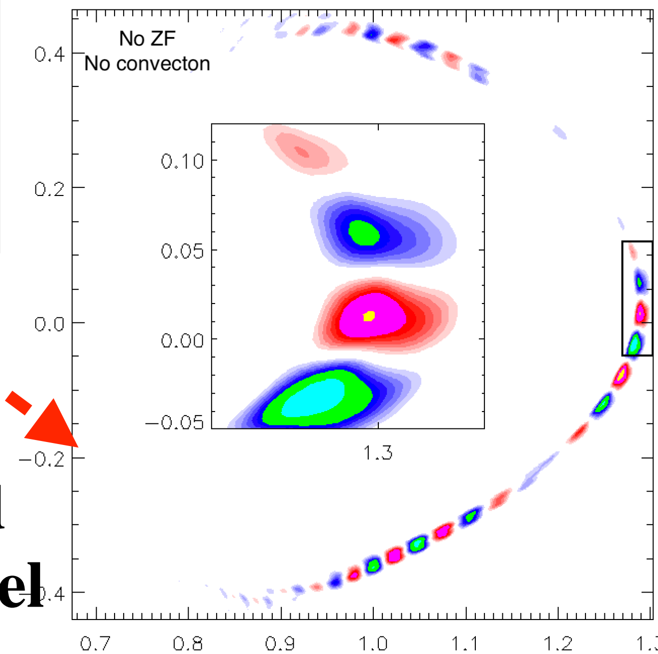

Mode shearing of ZF and convection partially cancel

Comparison of zonal fields spatial scale

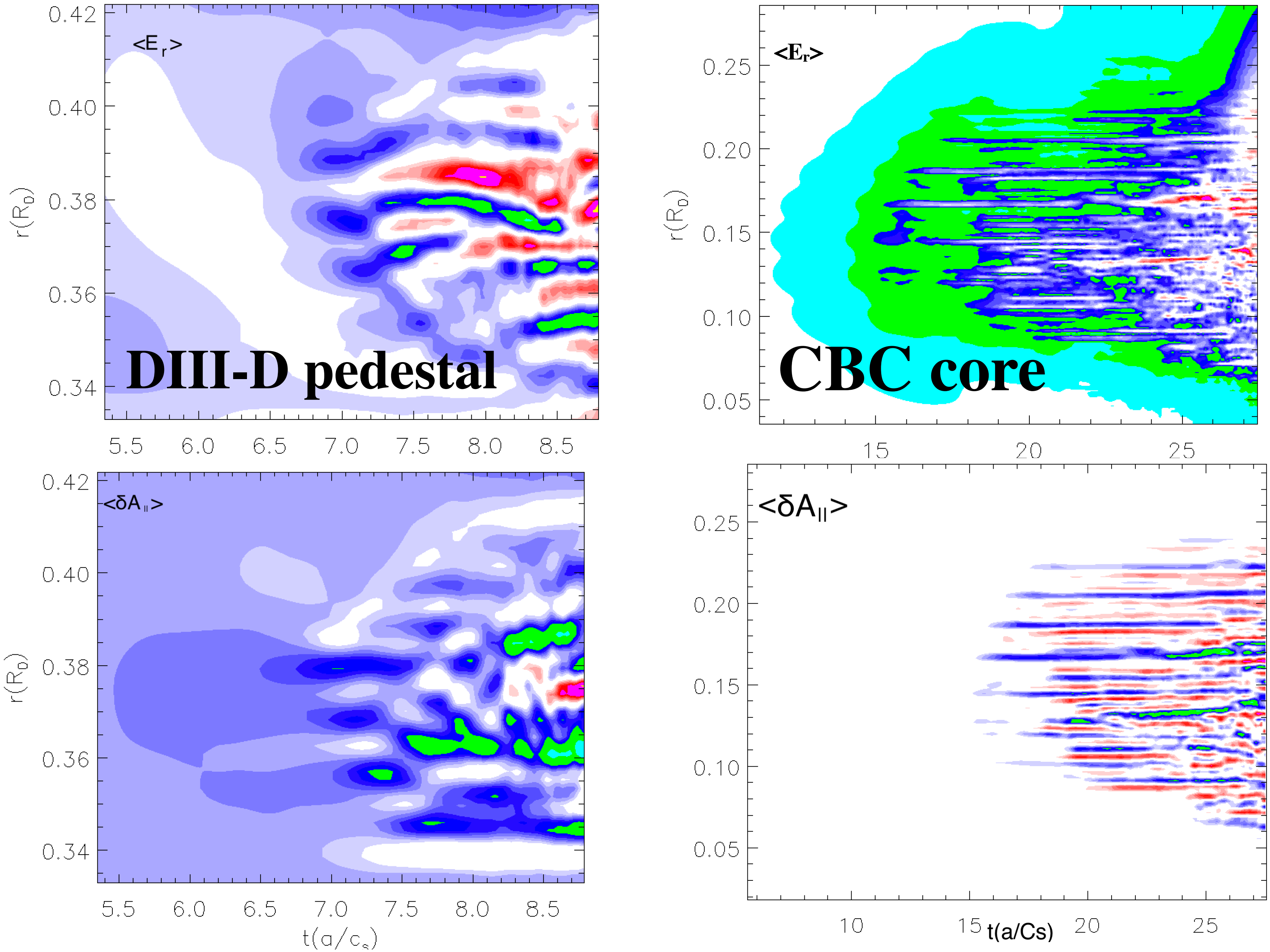

Conclusions

- Global gyrokinetic simulation results of nonlinear KBM show that KBM can be nonlinearly regulated and saturated by the zonal fields, including the zonal flow and the zonal current.

- An intermediate regime resembling that discovered in full MHD simulations is observed. Current sheet thinning can destabilize tearing modes.

- At the narrow pedestal region, zonal fields shearing scale is small, and its effects can be suppressed to some extent by the non-zonal nonlinear convection.

Disruptive problems are complex in nature and involve coupling of multi physical mechanisms —— Machine Learning?

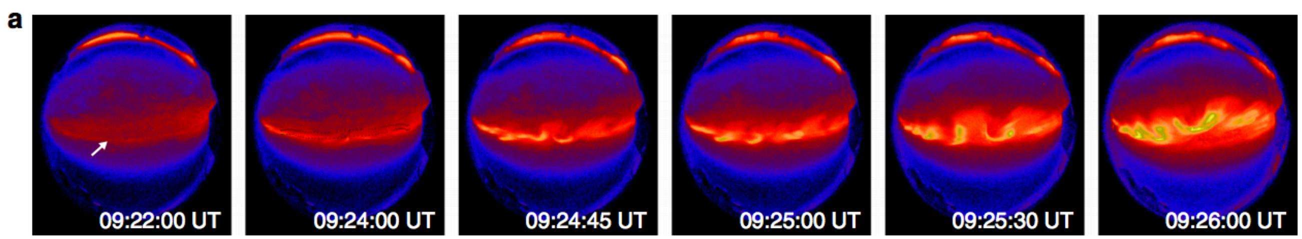

Avalanche?
Reconnection?
KBM?
KAW?

Substorm onset on Sep 2012 [Kalmoni 2018]

LCFS in Disruption [Sugihara 2007]

ELM Filaments in MAST

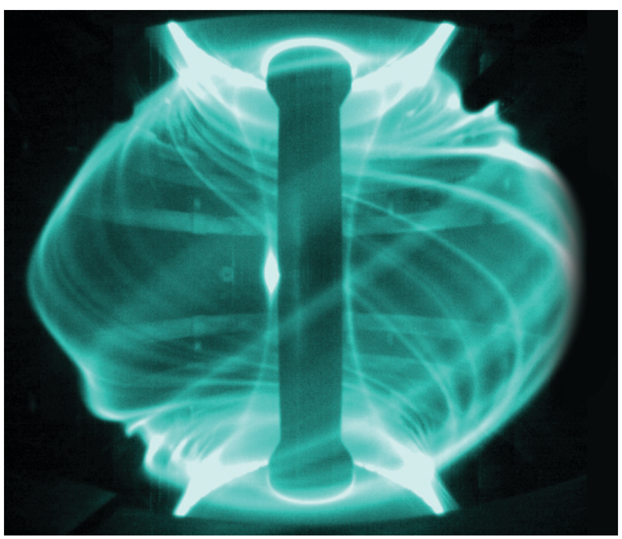

KBM?
MTM?
Resonance?

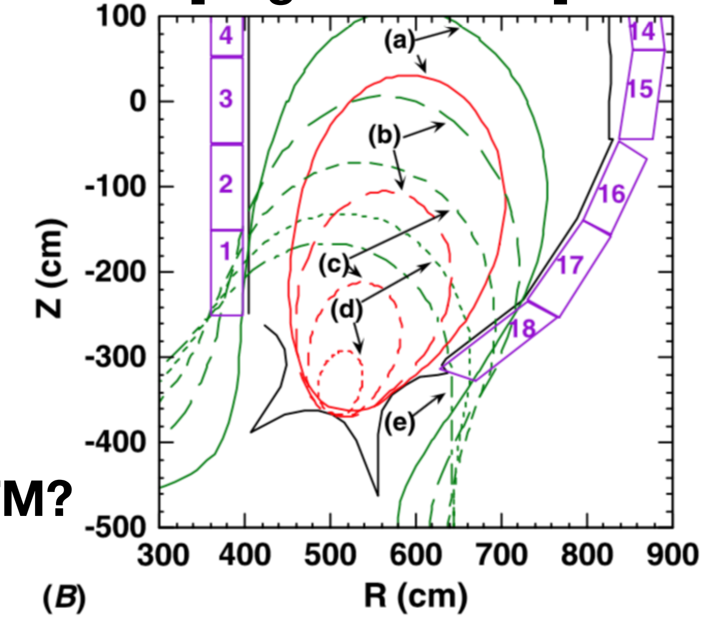

Avalanche?
NTM?
What drives NTM?

Machine Learning in disruption predictions (1996)

Effort since 90s. [J.V. Hernandez 1996]
1-2 layers of feedforward neural nets
2018: ~30 warning time, >90% Accuracy
SVM+Deep learning [Ferreira 2018]

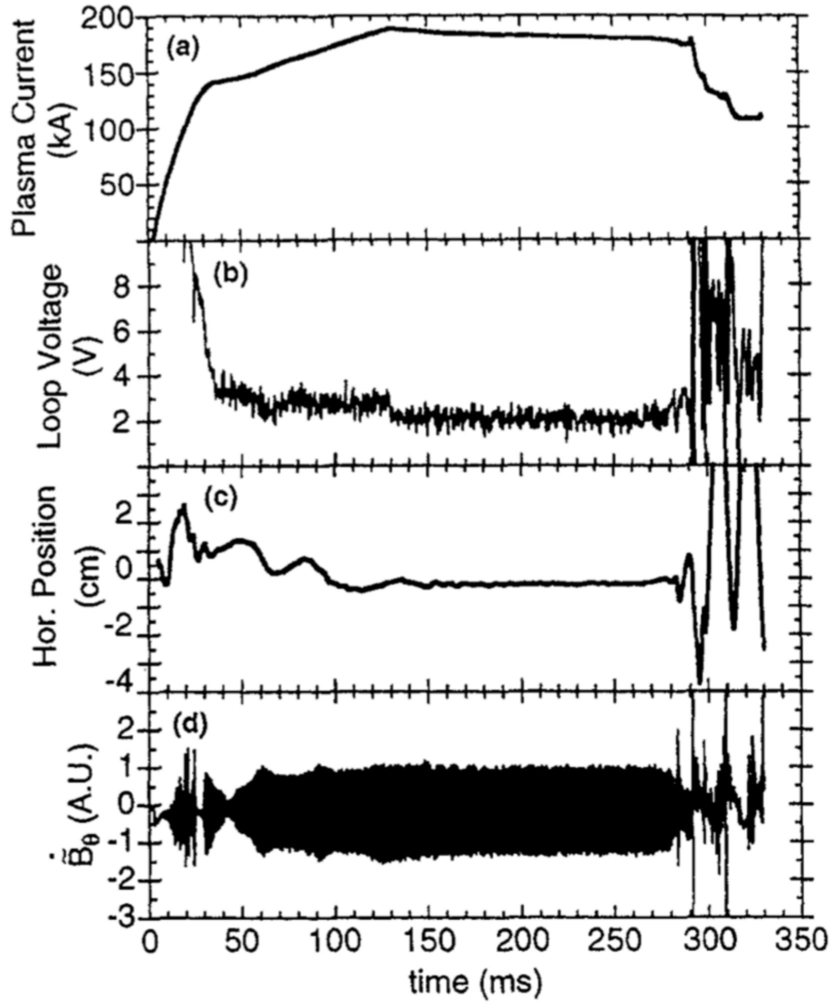

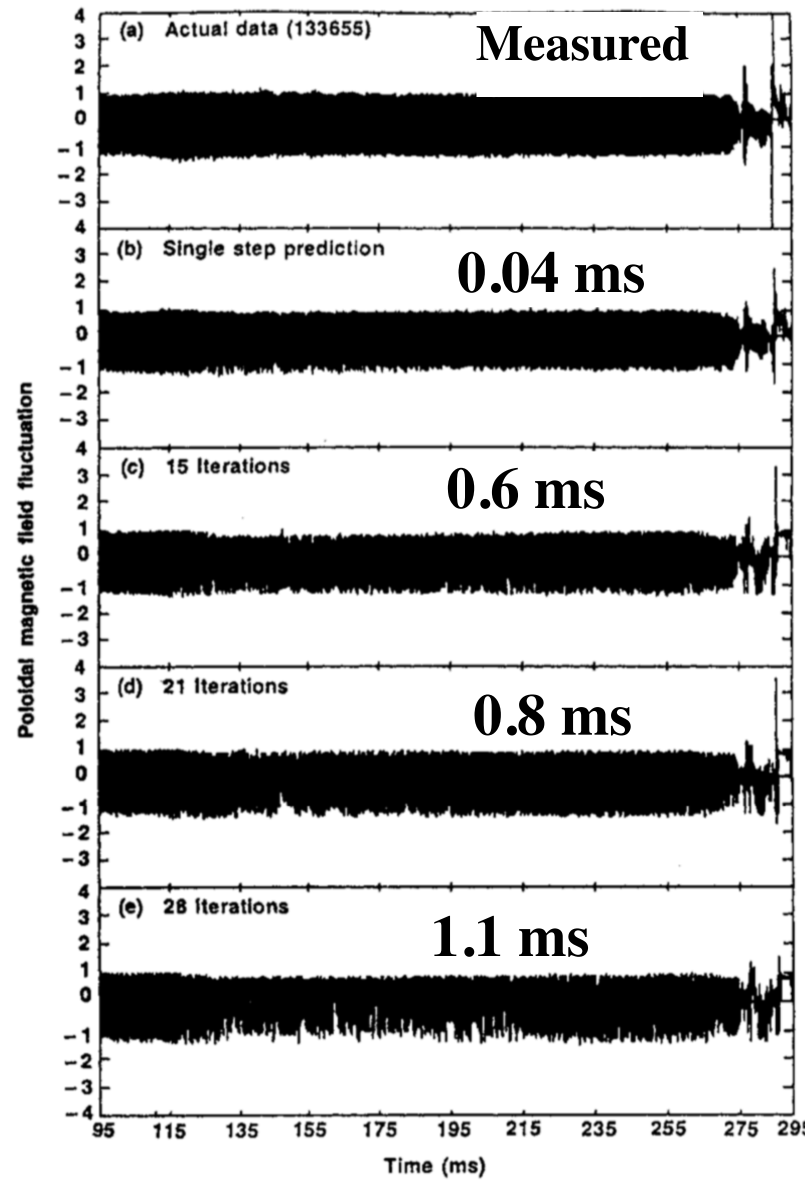

Machine Learning in disruption predictions (2005)

Cross-tokamak prediction is hard [C. Windsor 2005]
Two layer Neural Network
JET <—> ASDEX Upgrade (< 70% , 10ms)

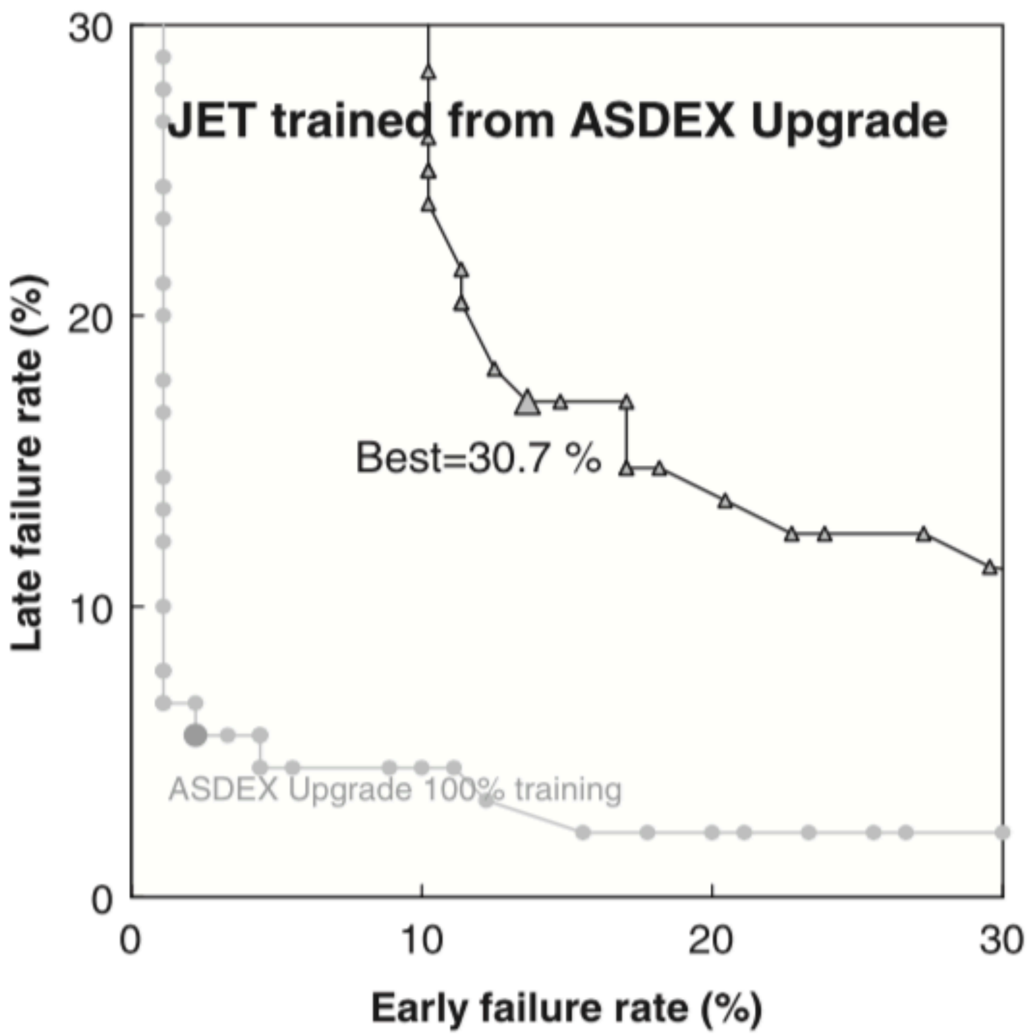

Machine Learning in disruption predictions (2018)

Some 'adaptivity' achieved. [A. Murari 2018]
Probabilistic SVM

Average warning time longer than 300ms (~95% True Positive, 5% False Positive)

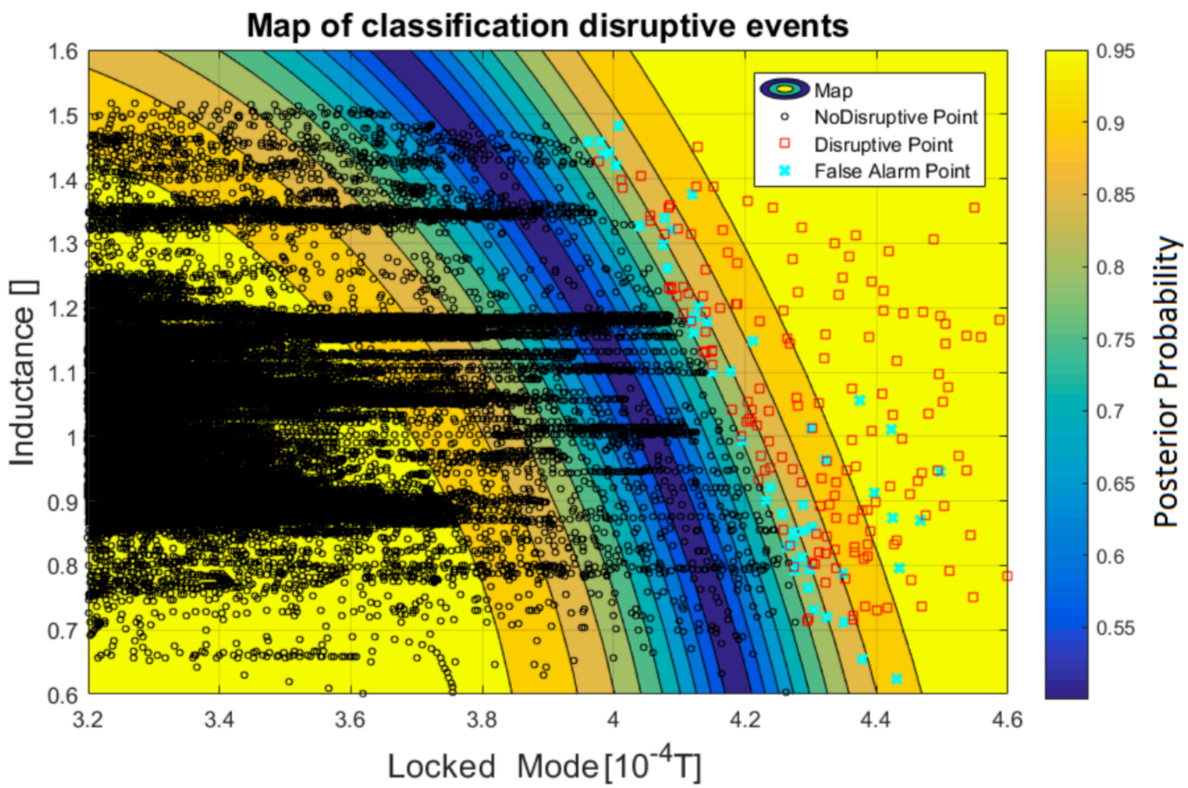

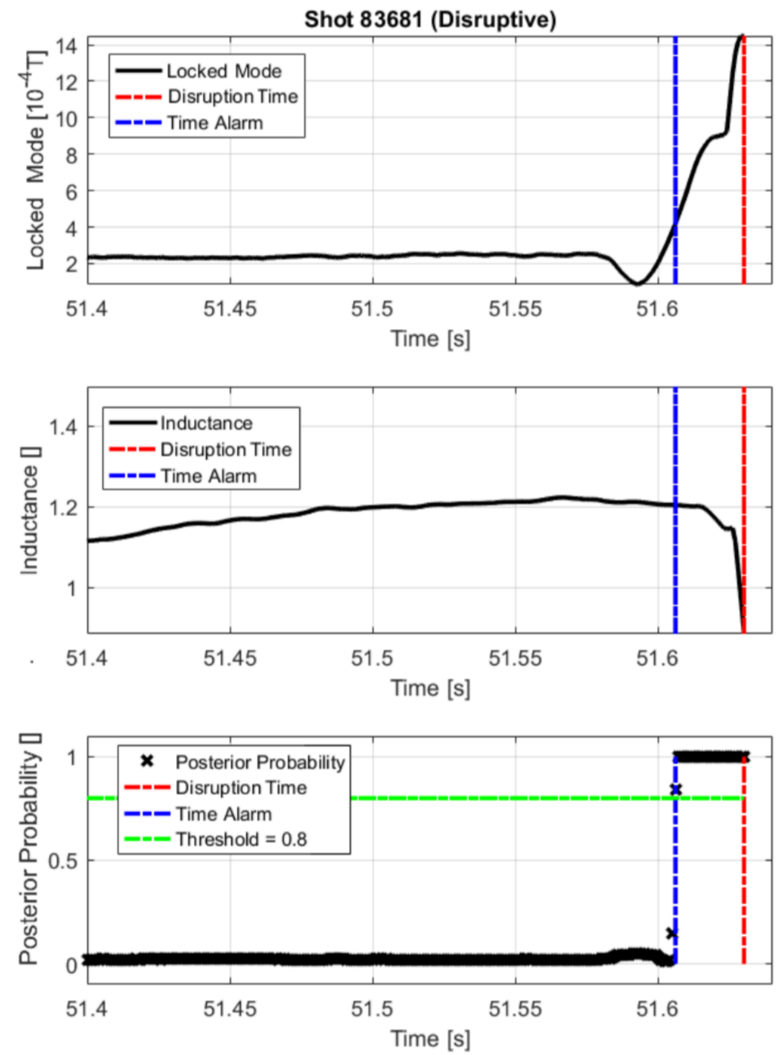

Deep Learning vs "Shallow" Learning

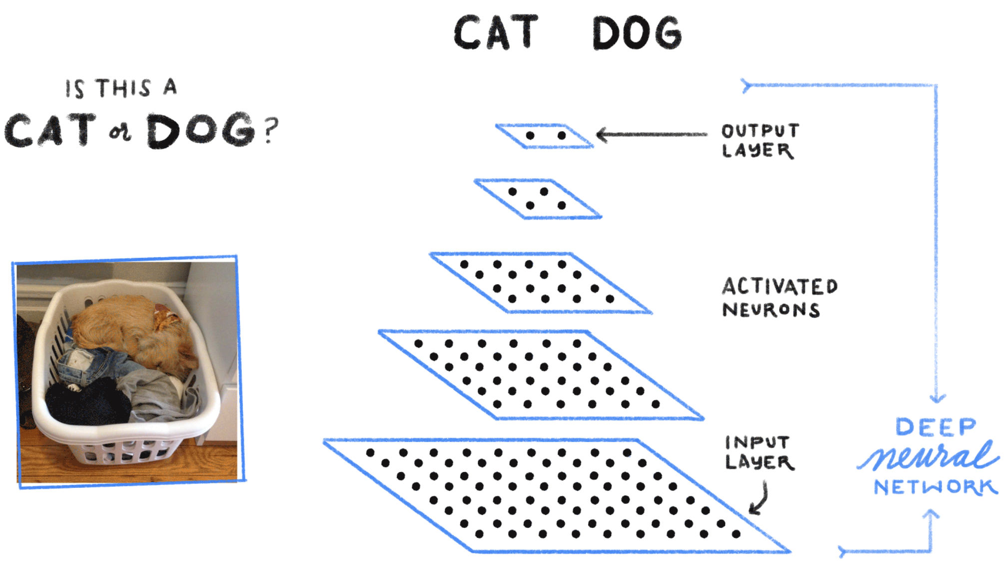

Hierarchical representation of Complex data

Deep RNNs -> handwriting/ speech recognition
Deep CNNs-> image recognition/ AlphaGo

Q: Is this going to disrupt?

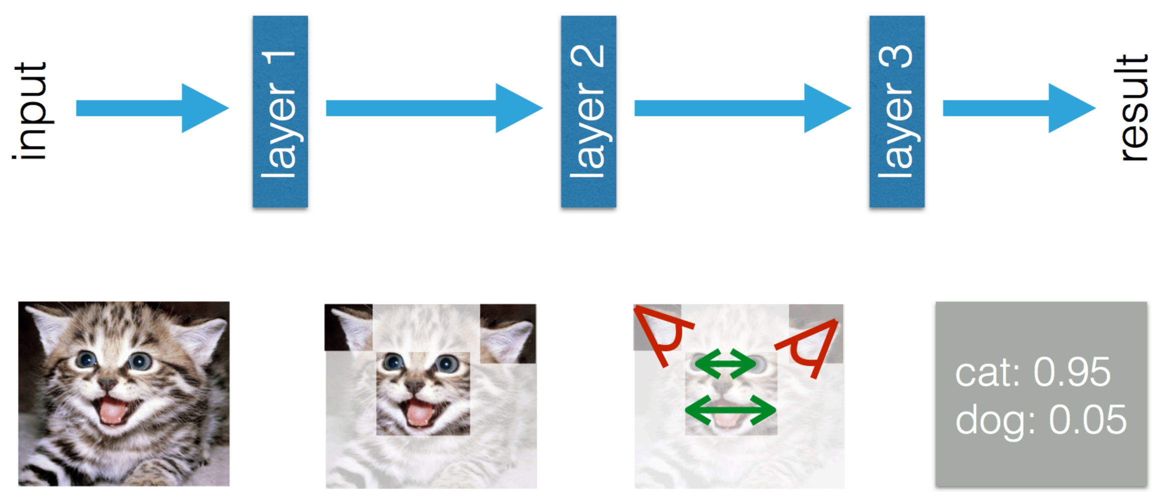

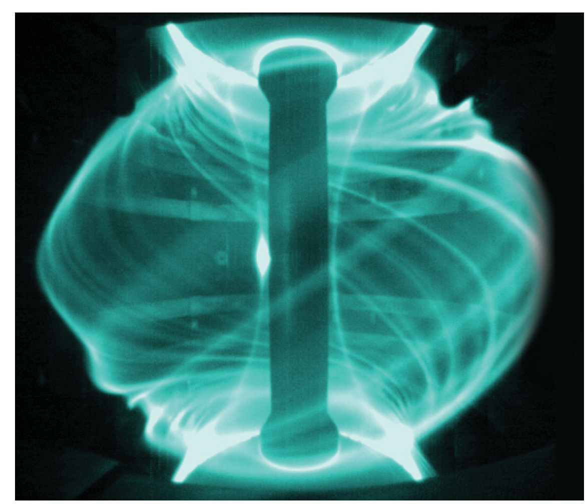

Deep Learning — CNNs

Superhuman performance of Go game
Image recognition

Example: Cifar10 data
10 classes, 60000
32X32 images
Error rate <2% (2018)

Parsimonious parameterization

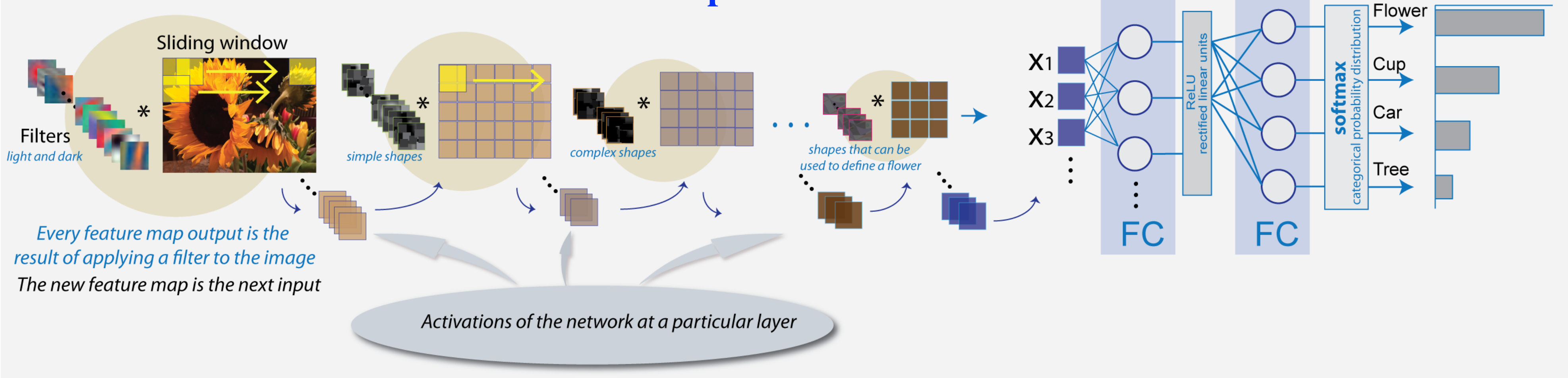

Cat is always a cat

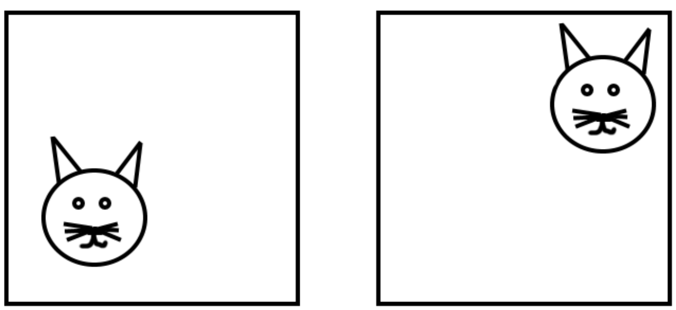

Translational Invariance

Certain island always cause disruption

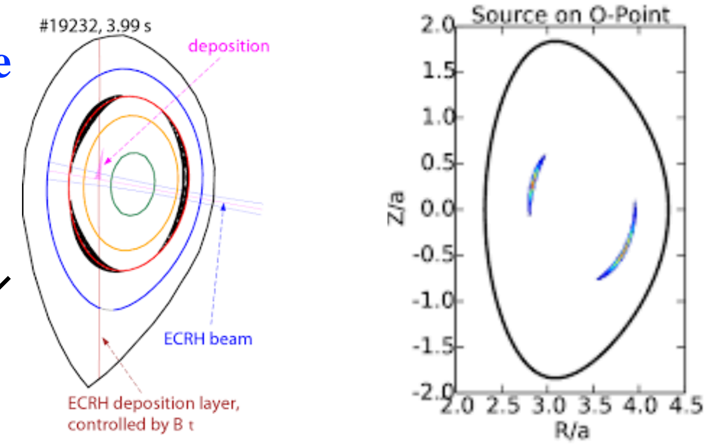

Q: But how can we get these detailed data?

Q: But how can we get these detailed data?

— First-Principles-Simulation results as virtual experimental results

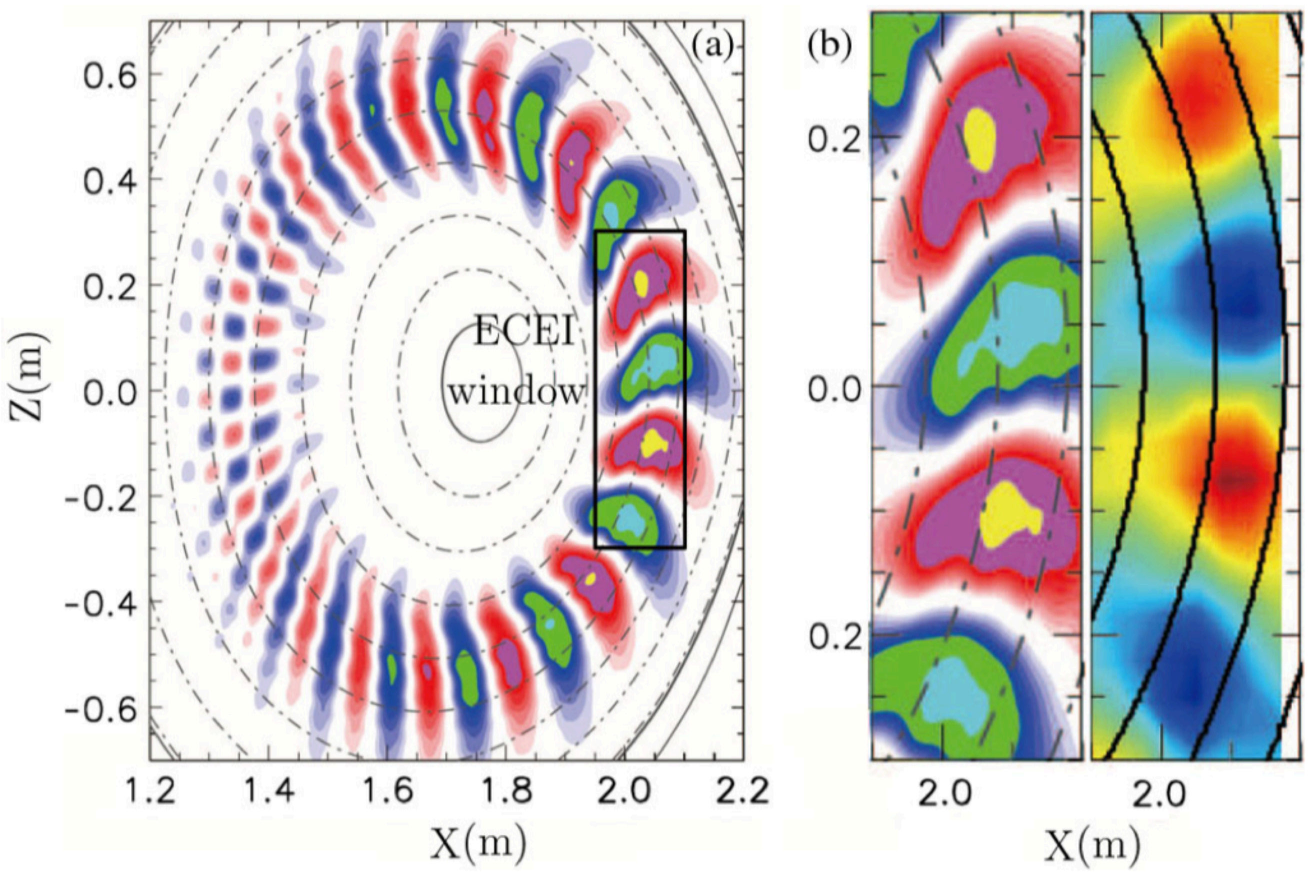

Linear Properties (Useful even in simple regression models)

Complete particle/field information

Reproduce any diagnostic in real/ velocity space

Perfect 2/3 dimensional data for Neural Networks

Comparison of TAE Te structure from the simulation (left) and from the DIII-D experiment (right) in the ECEI window [Z. Wang, 2013]

Use machine learning to select input for first-principles codes

Hundreds of physical parameters in the code
What factor, which physics is more important to disruption?

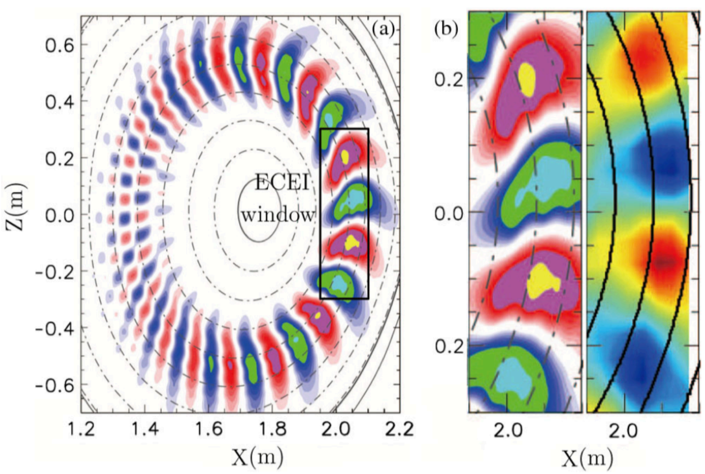

Feed as feature

Fix imbalanced data set

Deep Learning Model

Select sensitive parameters/
Extract useful phase space info
Reduce particle Noise

```
! physical unit for equilibrium
                              ! 1: Input reference flux surface (iflux) values for etemp0 and eden0
  etemp0=196.9 !150 !287.29          ! on-axis electron temperature, unit=ev
  eden0=1.496e14 !0.21e14 !0.4178e14        ! on-axis electron number density, unit=1/cm^3
  r0=177.1              ! major radius, unit=cm
  b0=16793.0            ! on-axis magnetic field, unit=gauss
 /

!!!!!!!!!!!!!!!!!!!!!!!!!!!!!!!!!!!!!!!!!!!!!!!!!!!!!!!!!!!!!!!!!!!!!!!!!!!!!!!!!!!!!!!!!!!!!!!!!!!!!!!!

&equilibrium_parameters

! example numerical/analytical equilibrium using variables from numereq=1

psiw_analytic= 3.75e-2         ! poloidal flux at wall
ped_analytic=  3.75e-2       ! poloidal flux at separatrix

! q and zeff profile is parabolic: q=q1+q2*psi/psiw+q3*(psi/psiw)^2
q_analytic=   0.8200  1.10000 1.00000  !
ze_analytic=  1.0  0.0  0.0   !
er_analytic=  -0.06312057  0.1661067  0.0   !

itemp0_analytic=  1.0         ! on-axis thermal ion temperature, unit=T_e0
ftemp0_analytic=  2.0         ! on-axis fast ion temperature, unit=T_e0
fden0_analytic=   1.0e-5      ! on-axis fast ion density, unit=n_e0
fetemp0_analytic= 1.0         ! on-axis fast electron temperature, unit=T_e0
feden0_analytic=  1.0         ! on-axis fast electron density, unit=n_e0
```

Produce physical results

Summary

- Deep learning could achieve break through in disruption research, with the help from first-principles based codes.

- The linear properties as well as nonlinear mode structures from the simulations could be incorporated into the deep learning models for disruption predictions in the form of a new parameter/channel, as a first-principles physics guide to the AI.

- The deep learning model could in turn provide feedback on the sensitivity of the parameters and thus automatically select new inputs for the first-principles codes.

Thank you!

Following Slides are Supplementary materials

Gyrokinetic simulation model

$$\frac{dw_\alpha}{dt} = (1-w_\alpha)\Bigg[-\left(v_\parallel\frac{\delta\mathbf{B}_\perp}{B_\parallel^*} + \mathbf{v}_E + \mathbf{v}_{b\parallel} + \mathbf{v}_{NL}\right)\cdot\boldsymbol{\kappa}_\alpha + \frac{u_{\parallel\alpha 0}\delta\mathbf{B}_\perp}{T_{\alpha 0}B_0}\cdot\nabla(\mu B_0 + Z_\alpha\Phi_{eq})$$

$$-\frac{v_\parallel\delta\mathbf{B}_\perp}{T_{\alpha 0}B_0}\cdot\nabla(Z_\alpha\Phi_{eq}) - \left[\mathbf{b_0}\cdot\nabla(Z_\alpha\phi + Z_\alpha\phi_{NL} + \mu\delta B_\parallel) + \frac{\partial\delta A_\parallel}{\partial t}\right]\frac{Z_\alpha(v_\parallel - u_{\parallel\alpha 0})}{T_{\alpha 0}}$$

$$-\frac{1}{T_{0\alpha}}\left(\mathbf{v_g} + \left(\frac{v_\parallel\delta\mathbf{B}_\perp}{B_\parallel^*} + \mathbf{v_c} + \mathbf{v_{deq}}\right)\left(1-\frac{u_{\parallel\alpha 0}}{v_\parallel}\right)\right)\cdot\nabla(Z_\alpha\phi + Z_\alpha\phi_{NL} + \mu\delta B_\parallel)\Bigg]$$

$$\frac{\partial\delta n_e}{\partial t} + \mathbf{B_0}\cdot\nabla\left(\frac{n_0\delta u_{\parallel e}}{B_0}\right) + B_0\mathbf{v_E}\cdot\nabla\left(\frac{n_0}{B_0}\right) - n_0(\mathbf{v}_* + \mathbf{v_E})\cdot\frac{\nabla B_0}{B_0}$$

$$+\delta\mathbf{B}_\perp\cdot\nabla\left(\frac{n_0 u_{\parallel 0}}{B_0}\right) + \frac{c\nabla\times\mathbf{B_0}}{eB_0^2}\left(-\nabla\delta P_\parallel - \frac{(\delta P_\perp - \delta P_\parallel)\nabla B_0}{B_0} + n_0 e\nabla\delta\phi\right)$$

$$+\delta\mathbf{B}_\perp\cdot\nabla\left(\frac{n_{0e}\delta u_{\parallel e}}{B_0}\right) + B_0\mathbf{v}_E\cdot\nabla\left(\frac{\delta n_e}{B_0}\right) + \frac{c\delta n_e}{B_0^2}\mathbf{b}_0\times\nabla B_0\cdot\nabla\phi + \frac{c\delta n_e}{B_0^2}\nabla\times B_0\cdot\nabla\phi$$

$$+\frac{c\mathbf{b_0}\times\nabla\delta B_\parallel}{e}\nabla\left(\frac{\delta P_\perp + P_{\perp 0}}{B_0^2}\right) + \frac{c\nabla\times\mathbf{b_0}\cdot\nabla\delta B_\parallel}{eB_0^2}(\delta P_\perp + P_{\perp 0}) = 0$$

$$\frac{\partial\delta A_\parallel^A}{\partial t} = c\mathbf{b}_0\cdot\nabla\phi_{ind}.$$

$$\delta n_e^{(a)} = n_0\left(\frac{e\delta\phi + e\delta\phi_{ind}}{T_e} - \frac{\delta B_\parallel}{B_0}\right) + \frac{\partial n_0}{\partial\psi_0}\delta\psi + \frac{\partial n_0}{\partial\alpha_0}\delta\alpha$$

$$\boxed{\left(\nabla_\perp^2 - \frac{\omega_{pe}^2}{c^2}\right)\frac{\partial\delta A_\parallel^{NA}}{\partial t} = \frac{\omega_{pe}^2}{c}\chi_\parallel - c\nabla_\perp^2(\mathbf{b}_0\cdot\nabla\phi_{ind})}$$

$$\frac{e\delta\phi}{T} = (1-\rho_s^{-2}\nabla_\perp^{-2})\frac{\delta n_i - \delta n_e}{n_0}$$

$$\frac{\delta B_\parallel}{B_0} = \frac{\beta}{2}\left[-\frac{\delta P_e + \delta\tilde{P}_i}{P_0} + \frac{\delta n_i - \delta n_e}{n_0} + (1-\rho_s^2\nabla_\perp^2)^{-1}\frac{\delta n_i - \delta n_e}{n_0}\right]$$

GTC Flow Chart-Conservative

$$\delta f_i^n,\ \delta n_e^n,\ \delta\phi^n,\ \delta\phi_{ind}^n,\ \delta A_\parallel^{A,n}$$
$$\delta A_\parallel^{NA,n},\ \delta B_\parallel^n,\ \delta h_e^n,\ \delta u_{e\parallel}^n$$

$$\delta f_i^{n+1} = \frac{\partial f_i}{\partial t}\left(\delta\phi^n, \delta\phi_{ind}^n, \delta B_\parallel^n, \delta A_\parallel^{A,n}, \delta A_\parallel^{NA,n}\right)\Delta t + \delta f_i^n$$

$$\delta n_e^{n+1} = \frac{\partial\delta n_e}{\partial t}\left(\delta u_{e\parallel}^n, \delta\phi^n, \delta\phi_{ind}^n, \delta B_\parallel^n, \delta A_\parallel^{A,n}, \delta A_\parallel^{NA,n}\right)\Delta t + \delta n_e^n$$

$$\delta A_\parallel^{A,n+1} = \frac{\partial\delta A_\parallel^A}{\partial t}\left(\delta\phi_{ind}^n\right)\Delta t + \delta A_\parallel^{A,n}$$

$$\delta A_\parallel^{NA,n+1} = \frac{\partial\delta A_\parallel^{NA}}{\partial t}\left(\delta u_{e\parallel}^n, \delta\phi^n, \delta\phi_{ind}^n, \delta B_\parallel^n, \delta A_\parallel^{A,n}, \delta A_\parallel^{NA,n}\right)\Delta t + \delta A_\parallel^{NA,n}$$

$$\delta h_e^{n+1} = \frac{\partial\delta h_e}{\partial t}\left(\frac{\partial\delta f_e^{(a),n}}{\partial t}, \delta\phi^n, \delta\phi_{ind}^n, \delta B_\parallel^n, \delta A_\parallel^{A,n}, \delta A_\parallel^{NA,n}\right)\Delta t + \delta h_e^n$$

$$\delta\phi_{ind}^{n+1} = \delta\phi_{ind}(\delta n^{n+1}, \delta\phi^{n+1}, \delta A_\parallel^{A,n+1})$$

$$\frac{\delta f^{(a),n+1}}{\partial t} = \frac{\delta f^{(a)}}{\partial t}\left(\frac{\partial\delta n_e^{n+1}}{\partial t}, \delta\phi_{ind}^{n+1}, \frac{\partial\delta B_\parallel^{n+1}}{\partial t}\right)$$

$$\delta u_{e\parallel}^{n+1} = \delta u_{e\parallel}(\delta A_\parallel^{A,n+1}, \delta A_\parallel^{NA,n+1}, \delta u_{i\parallel}^{n+1})$$

$$\delta B_\parallel^{n+1} = \delta B_\parallel(\delta P_e^{n+1}, \delta P_i^{n+1}, \delta\phi^{n+1})$$

$$\delta\phi^{n+1} = \delta\phi(\delta n_e^{n+1}, \delta n_i^{n+1}, \delta B_\parallel^{n+1})$$

Coupled Equation

$$\delta f_i^{n+1},\ \delta n_e^{n+1},\ \delta\phi^{n+1},\ \delta\phi_{ind}^{n+1},\ \delta A_\parallel^{A,n+1}$$
$$\delta A_\parallel^{NA,n+1},\ \delta B_\parallel^{n+1},\ \delta h_e^{n+1},\ \delta u_{e\parallel}^{n+1}$$

Comparison of ITG and KBM zonal flow generation

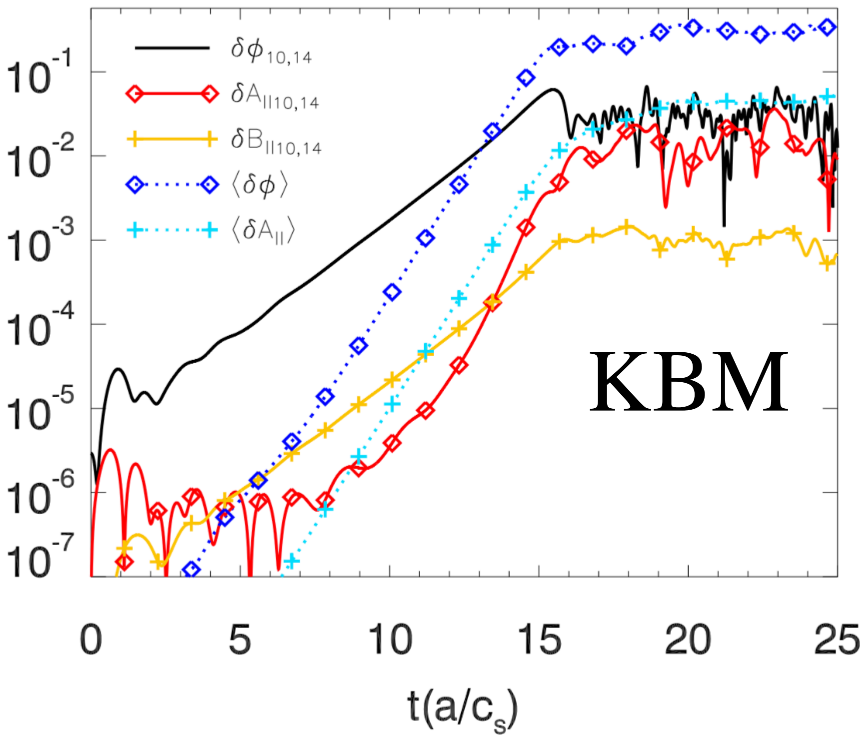

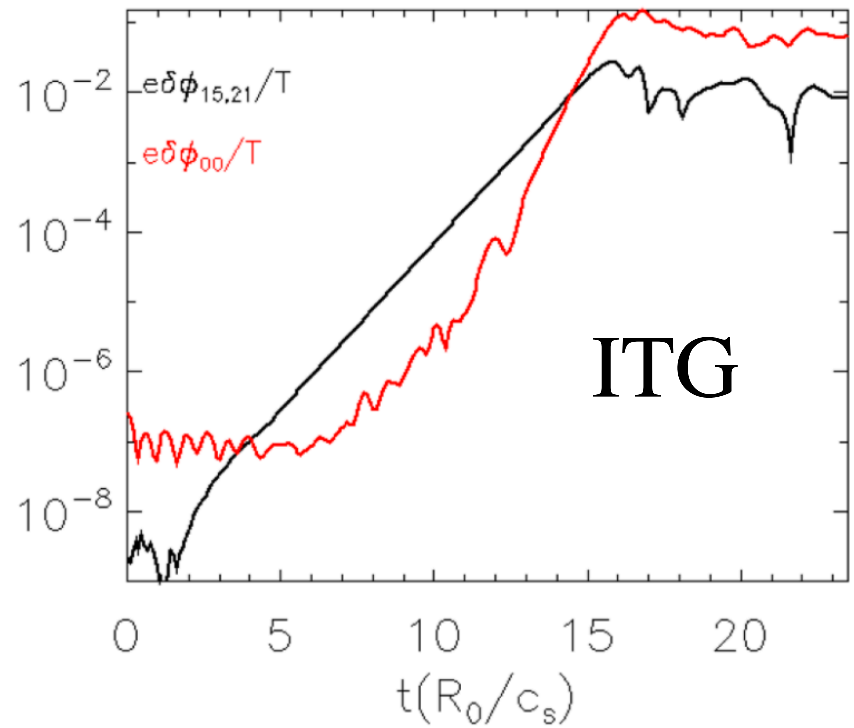

KBM nonlinear structure in later nonlinear regime in DIII-D edge

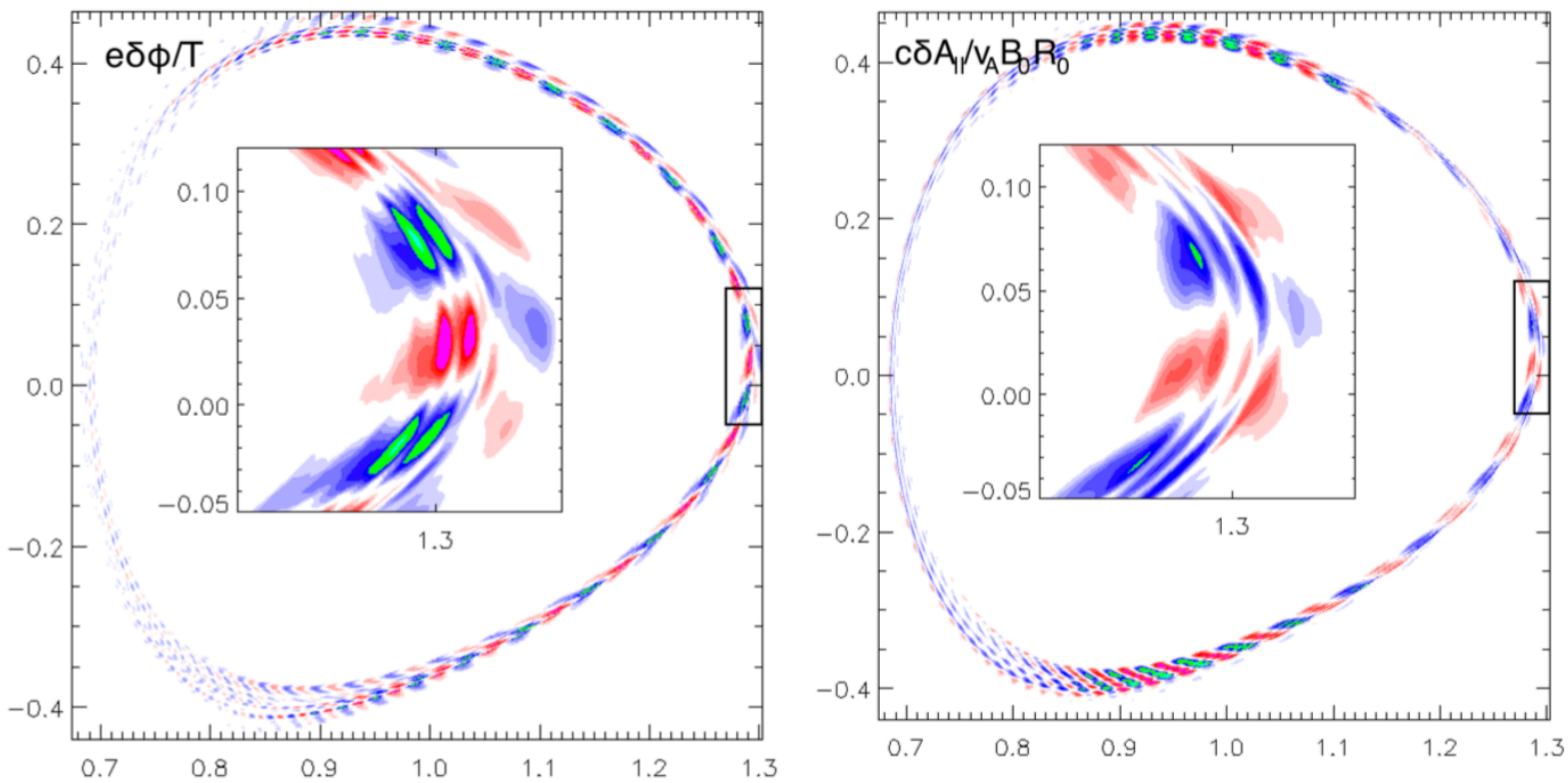

CBC case with resistivity

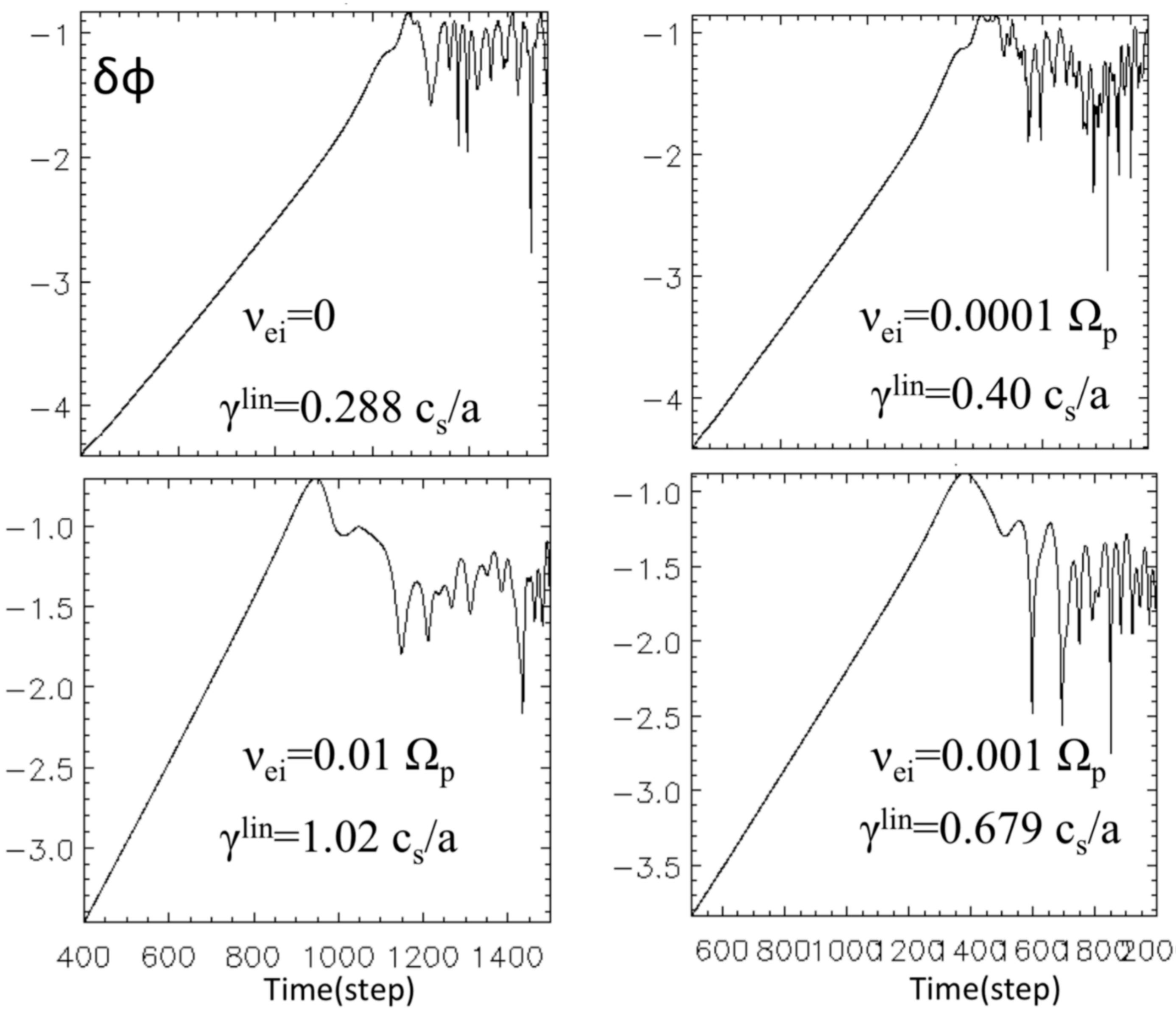

CBC case with resistivity